20.6 Solutions of Exercises of Chapter 11: FFAG, Scaling

20.6.1 A 150 MeV, Proton, Radial Sector FFAG

11.1

Field in a Radial Sector Dipole Triplet

(a) An input data file to simulate a 150 MeV scaling FFAG cell.

The input data file, including comments for guidance, is given in Tab. 20.68. Geometry and field data under FFAG are from Tab. 11.1, possibly slightly varied according to the purposes of subsequent questions.

(b) A graph of $B_Z(R,\theta)|_{Z=0}$ in a radial sector scaling FFAG dipole.

In view of generating the mid-plane field from raytracing outcomes, a set of 25 trajectories is launched, with initial coordinates Y_0, T_0, Z_0, P_0 and relative momentum $D_0 = p/p_{\rm ref}$, defined using OBJET[KOBJ=1] (Tab. 20.68). Initial radii Y_0 are evenly spaced over the useful field region, namely

$$Y_0 : r_1 \rightarrow r_{25},\ \text{step}\ \Delta r \qquad \text{with}\ r_1 = 446\,\text{cm},\ r_{25} = 518\text{cm},\ \Delta r = 3\,\text{cm}$$

This Y_0 range results from Eq. 11.8, given $k = 7.6$ (Tab. 11.1) and $R_0 = 540\,$cm (the choice of R_0 is arbitrary). As a mid-plane field is desired, axial motion is taken null, $Z_0 = 0$ and $P_0 = 0$. By means of CONSTY each paticle is forced to maintain constant radius throughout the dipole. Note that a 3D map of the vector field instead, $\mathbf{B}(R,\theta,Z)$, can be generated if desired, by adding a Z_0 sampling, as CONSTY also forces Z to maintain its initial value Z_0.

The integration step size along the reference arc R_0 is $\Delta s = 3^+$ cm, resulting in 94 steps over

$$\theta : \theta_1 \rightarrow \theta_{95},\ \text{step}\ \Delta\theta = \Delta s/R_0\,, \qquad \text{with}\ \theta_1 = 0,\ \theta_{95} = 30^\circ,\ \Delta\theta = 0.31915^\circ$$

with the 30° triplet sector opening including half-drifts on both sides to make up a cell (Fig. 11.11). In that manner, during the stepwise raytracing process, the mid-plane field $B_Z(r,\theta)$ is computed at particle locations which are made to coincide with the $N_r \times N_\theta = 25 \times 95$ nodes of a 2D meshing.

Note: although not necessary as far as the present question (b) is concenred, this meshing has been taylored to be uniform, and to exactly cover the 30 degree sector, in view of the next question.

The magnetic field vector experienced along the trajectory accross the dipoles is part of the particle data logged in zgoubi.plt during the stewise integration, as an effect of the flag FFAG[IL=2] (Tab. 20.68). A graph of $B_Z(r,\theta)$ data so obtained, read from zgoubi.plt, is given in Fig. 20.83.

(c) Generating a 2D mid-plane field map for TOSCA to handle.

Table 20.68 Simulation input data file SFFAGCell.inc: 150 MeV KEK FFAG dipole triplet cell, a 30 degree angular sector. The FFAG keyword allows defining up to 5 indepent dipoles in that $AT = 30^\circ$ angular sector, only three are needed for the present DFD triplet. CONSTY option allows to raytrace a set of trajectories on *constant radii*. The present input data file also defines the lattice cell segment #S_SFFAG150Cell to #E_SFFAG150Cell, for use in INCLUDEs in subsequent exercises

```
SFFAGCell.inc file. FFAG triplet cell of a 12-cell 150MeV ring.
'MARKER'  SFFAGProbFieldMap_S
 'OBJET'
1839.090113                                                    ! Rigidity, case of 150 MeV proton.
1
25 1 1 1 1 1                     ! This creates 25 trajectories, corresponding to as many radial steps,
3. 0. 0. 0. 0. 0.                   ! whereas theta-steps result from the integration step size, below.
482. 0.  0.  0. 0.  1.           ! Yo is taken half-way between a minimum 442 cm (injection region) and
!                                                          a maximum 516 cm (extraction region).
'OPTIONS'
1 1
CONSTY ON                                ! Forces particles on Y=Yo and Z=Zo, in subsequent raytracing.

'MARKER'  #S_SFFAG150Cell
'FFAG'
2    ! Set IL=2 to store particle and field data along trajectories (in zgoubi.plt) for further plotting.
3   30.  540.           ! Number of dipoles over AT; AT=tetaF+2tetaD+2Atan(XFF/R0); reference radius R0.
6.465  0.  -12.1744691  7.6                  ! Dipole 1 (D type): ACNT; unused; B0; geometrical index k.
6.3   3.     ! EFB 1 : lambda~gap size; kappa=gap shape index: detemines radius-dependent fringe extent.
4  .1455   2.2670  -.6395  1.1558  0. 0.  0.
1.715 0.    1.E6  -1.E6  1.E6  1.E6
6.3   3.     ! EFB 2 : lambda~gap size; kappa=gap shape index: detemines radius-dependent fringe extent.
4  .1455   2.2670  -.6395  1.1558  0. 0.  0.
-1.715  0.    1.E6  -1.E6  1.E6  1.E6
0. -1                                                                  !  EFB 3 : inhibited by iop=0.
0  0. 0. 0. 0. 0. 0. 0.
0  0. 0. 0. 0. 0. 0. 0.
15.   0.   16.9055873  7.6                       ! Dipole 2 (F type): the pattern repeats a first time.
6.3   3.     ! EFB 1 : lambda~gap size; kappa=gap shape index: detemines radius-dependent fringe extent.
4  .1455   2.2670  -.6395  1.1558  0. 0.  0.
5.12   0.    1.E6  -1.E6  1.E6  1.E6
6.3   3.     ! EFB 2 : lambda~gap size; kappa=gap shape index: detemines radius-dependent fringe extent.
4  .1455   2.2670  -.6395  1.1558  0. 0.  0.
-5.12   0.    1.E6  -1.E6  1.E6  1.E6
0. -1
0  0. 0. 0. 0. 0. 0. 0.
0  0. 0. 0. 0. 0. 0. 0.
23.535  0.  -12.1744691  7.6                     ! Dipole 3 (D type): the pattern repeats a second time.
6.3   3.     ! EFB 1 : lambda~gap size; kappa=gap shape index: detemines radius-dependent fringe extent.
4  .1455   2.2670  -.6395  1.1558  0. 0.  0.
1.715 0.    1.E6  -1.E6  1.E6  1.E6
6.3   3.     ! EFB 2 : lambda~gap size; kappa=gap shape index: detemines radius-dependent fringe extent.
4  .1455   2.2670  -.6395  1.1558  0. 0.  0.
-1.715  0.    1.E6  -1.E6  1.E6  1.E6
0. -1                                                                 ! EFB 3 : lateral face, unused.
0  0. 0. 0. 0. 0. 0. 0.
0  0. 0. 0. 0. 0. 0. 0.
0 2 ! Field computation analytic, 2nd order (take KIRD=2, 25 or 4 for flying grid interpolation instead).
3.0079078598 ! Integration step size: it determines angular step=3.007907/R0*30[deg], and thus the number
2 0. 0. 0. 0.   ! of integration steps along the 30 deg sector. USE 1~2cm RATHER, FOR MULTITURN TRACKING.
'MARKER'  #E_SFFAG150Cell

'SYSTEM'
2                                                              ! A 'call system' for next 2 commands:
gnuplot < ./gnuplot_Zplt_fieldMap.gnu                ! plot field data logged in / read from zgoubi.plt;
! okular gnuplot_Zplt_fieldMap.eps &                           ! view graph - requires a .eps viewer.

'MARKER'  SFFAGProbFieldMap_E
 'END'
```

---

gnuplot script gnuplot_Zplt_fieldMap.gnu, for Fig. 20.83:

```
#gnuplot_Zplt_fieldMap.gnu
set xlabel 'X [cm]' ; set ylabel 'Y [cm]' ; set zlabel 'B [kG]' ; set hidden3d
# Plot field:
splot "zgoubi.plt" u ($10*cos($22)):($10*sin($22)<520? $10*sin($22):1/0):($25) w p pt 5 ps .8 lc palette notit; pause 1
# Plot field data:
set size ratio -1; plot "zgoubi.plt"  u ($10*cos($22)):($10*sin($22))  with p pt 4 ps .2  notit
```

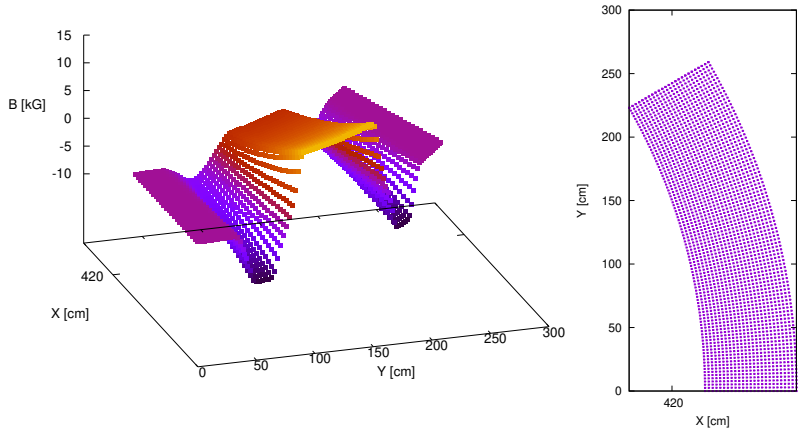

Fig. 20.83 Using the analytical field model provided by the FFAG keyword (Eq. 11.7), the 2D mid-plane field of KEK 150 MeV DFD dipole triplet is produced (left), over a uniform 2D polar meshing (right) defined by the particle sampling (Δr sampling) under OBJET and by the step size FFAG[XPAS] ($\Delta\theta$ sampling)

A straightforward way to generate a field map for TOSCA is to get field data on a uniform 2D mesh from the raytracing, *i.e.* from zgoubi.plt proper. Otherwise an intermediate step would be necessary, to interpolate from stepwise particle data onto a uniform meshing as required by TOSCA.

This has been accounted for in the input data file for the previous question, Tab. 20.68: the radial increment ΔR was defined to be constant using OBJET[KOBJ=1]. The angular increment $\Delta\theta = (\pi/6)/94$[steps] is constant by definition; what matters, and accounted for in (b), is ensuring that the first step (the upstream end of the mesh) is on the entrance border and the last step (downstream end of the mesh) on the exit border of the 30 degree sector: this was ensured taking an integration step size $XPAS = R_0[540\,\text{cm}] \times (\pi/6)/94[\text{steps}] = 3.0079078598\,\text{cm}$.

From this, it results evenly distributed $(R_{\text{i,j}}, \theta_{\text{i,j}})$ particle locations during the raytracing; step-by-step particle data logged in zgoubi.plt include coordinates and the field values $B_Z(R_{\text{i,j}}, \theta_{\text{i,j}}, Z = 0)$, they are read to be re-written in an ascii file with proper formatting for TOSCA to handle and track through.

Questions 4.1, 5.1 and their solutions may be resorted to in working out the details of the present question. This is left to the reader.

11.2

Orbits, Scalloping

(a) Periodic orbits.

The input data file in Tab. 20.69 produces 10 closed orbits consecutively (FIT finds them, one afte the other) for as many different momenta (REBELOTE repeats the sequence for a different momentum) ranging in (relative to $p_{\mathrm{ref}} = 551.345\,\mathrm{MeV/c}$, 150 MeV proton) p/p_{ref} : $0.2730426 \rightarrow 1.168858$ (12 to 200 MeV).

The input data file ends with a SYSTEM command which requests the two graphs dispayed in Fig. 20.84.

Table 20.69 Simulation data file to find the closed orbit for a set of different momenta. The INCLUDE grabs the FFAG dipole triplet segment defined in Tab. 20.68

```
Orbit scan.
'MARKER'  SFFAGProbOrbits_S                                              ! Just for edition purposes.
'OBJET'
1839.090113                                                  !  Reference rigidity (150MeV proton).
2
1  1
445.234  0.  0.  0. 0.  0.273042677097  'o'       ! 12MeV, Brho=502.1500877. To=0 due to sector geometry.
1
'PARTICUL'
938.27231  1.60217733D-19 0. 0. 0.                                      ! PROTON would do as well.

'INCLUDE'                                                 ! Include the 30 degree sector dipole triplet,
1                                                                      ! within dedicated  LABEL1s.
./SFFAGCell.inc[#S_SFFAG150Cell:#E_SFFAG150Cell]

 'FIT2'
1
2 30 0  2.
2  1e-9 99                                                      ! A penalty value controls the accuracy
3.1 1 2 #End 0. 1. 0                                      ! of the convergence to periodic coordinates.
3.1 1 3 #End 0. 1. 0                                          ! 3.1 is the constraint for periodicity.
 'MARKER' afterFIT                                                     ! FAISTORE above applies here.

'REBELOTE'                                                            ! Repeat the previous sequence,
10 0.1 0  1                                                    ! 10 times; prior to repeating, change
1                                                      ! 1 parameter, namely parameter 35 under OBJET: the
OBJET 35 0.27304263798:1.1688582876       ! relative momentum D=p/p_ref, in the range 0.27304...:1.16...

'SYSTEM'
3
gnuplot < ./gnuplot_Zplt_XY.gnu                 ! Call  gnuplot scripts once that tracking is completed.
gnuplot < ./gnuplot_Zplt_XB.gnu
gnuplot < ./gnuplot_Zplt_orbits.gnu

'MARKER'  SFFAGProbOrbits_E                                              ! Just for edition purposes.
 'END'
```

gnuplot scripts for the graphs of Fig. 20.84 (excerpt):

```
# gnuplot <./gnuplot_Zplt_XY.gnu
set xlabel "{/Symbol q} [deg]" ; set ylabel "R [m]"; r2d = 180./ (4.*atan(1.)) ; cm2m = 0.01 ; npass=11 ; FITlast=1
plot for [FITnb=2:npass] 'zgoubi.plt' u \
($49==FITnb && $51==FITlast ? $22*r2d :1/0):($10*cm2m):($49) w p pt 4 ps .2 lc palette notit ; pause 1

# gnuplot <./gnuplot_Zplt_XB.gnu
set xlabel "{/Symbol q} [deg]" ; set ylabel "R [m]"; r2d = 180./ (4.*atan(1.)) ; kG2T= 0.1 ; npass=11 ; FITlast=1
plot for [FITnb=2:npass] 'zgoubi.plt' u \
($49==FITnb && $51==FITlast ? $22*r2d :1/0):($25 *kG2T):($49) w l lc palette notit ; pause 1
```

gnuplot script for Fig. 20.85 (excerpt):

```
# ./gnuplot_Zplt_orbits.gnu
set size ratio 1 ; set polar; pi = 4.*atan(1.) ; set grid polar 2*pi/12. ; cm2m = 0.01 ; Ncell = 12 ; FITLast=1
plot  for [i=1:Ncell] "zgoubi.plt" u ($51==FITLast ? $22 +(i-1)*2*pi/Ncell :1/0):(cm2m* $10)  w p pt 6 ps .09 notit
```

gnuplot script for Fig. 20.86:

```
# gnuplot_Rovrho.gnu
set xlabel "{/Symbol q} [deg]" ; set ylabel "R/{/Symbol r}" ; r2d = 180./ (4.*atan(1.)) ; npass=11 ; FITlast=1
plot for [FITnb=2:npass] 'zgoubi.plt' u ($49==FITnb && $51==FITlast && ($22*r2d>12 && $22*r2d<18) ? \
  $22*r2d :1/0):($10 / ($40*(1.+$2)/$25)) w lp ps .6 notit; pause 1
# Replace  '($10 / ($40*(1.+$2)/$25))'  by  '($40*(1.+$2)/$25'  for \rho(\theta) graph.
```

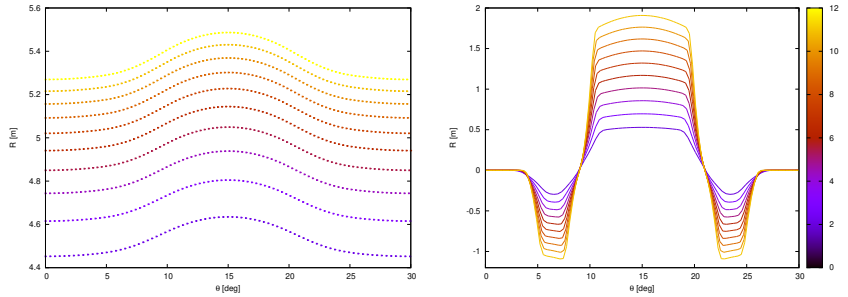

Fig. 20.84 Left: orbit scalloping across the AT=30° angular extent encompassed in FFAG keyword simulation, for 10 different proton energies ranging in 12-200 MeV (from bottom, smaller radius, to top, greater radius). Right: field experienced along these orbits, increasing with radius

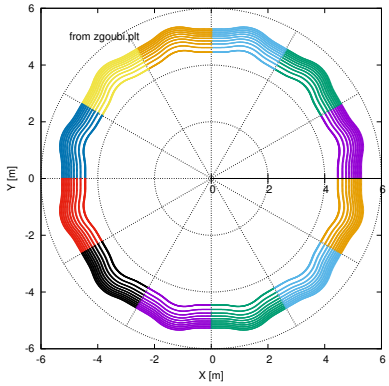

Fig. 20.85 Ten closed orbits, from 12 to 200 MeV, around the 12-cell radial sector FFAG ring

(b) Homothetic orbits.

Homothetic orbits around the ring, obtained from the previous question, read from zgoubi.plt, are plotted in Fig. 20.85.

It is found from Fig. 20.84 that the scalloping is about $0.2/5.4 \approx 3.7\%$ for the high energy closed orbit, about $0.2/4.5 \approx 4.4\%$ for the low energy closed orbit.

The similarity ratio $\frac{R}{\rho}(B\rho)$ is expected to be close to constant, within a few %, so justifying the assumption of Eq. **??**: $\phi \approx 0$ or equivalently $R \approx \overline{R}$. It can be computed for these 10 different rigidities: orbit radius R and field B_Z in the region $\theta \approx 15°$ are read from the step by step $R(\theta)$, $B_Z(\theta)$ data logged in zgoubi.plt, the latter yielding $\rho(\theta = 15°) = B\rho/B(\theta = 15°)$. Results are displayed in Fig. 20.86.

(c) Orbit excursion.

Figure 20.87 displays the numerical and theoretical (Eq. 11.8) values of the average orbit radius, they appear in good accord. It results from this that Eq. 11.11 is satisfied, with similar accuracy, $\approx 1\%$.

(d) Orbit scalloping

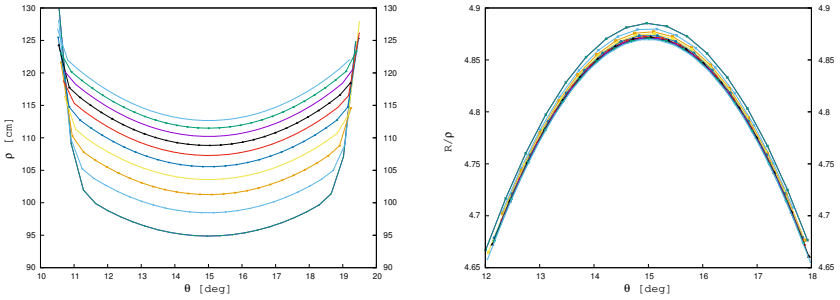

Fig. 20.86 Left: curvature radius $\rho(\theta)$ across the focusing dipole of the DFD triplet, for ten closed orbits in the energy range $12 < E < 200$ MeV. Right: $R/\rho(\theta)$ in the central region of the focusing dipole; the variation is $\approx \pm 0.1/4.75 = \pm 2‰$

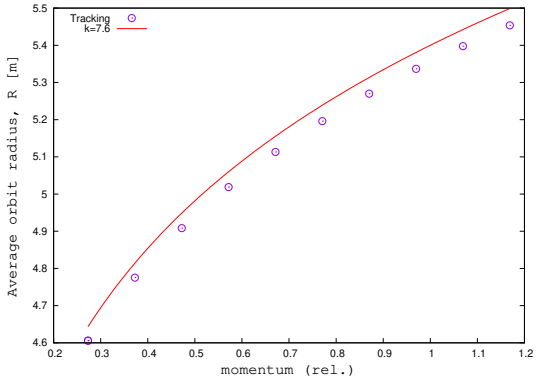

Fig. 20.87 Dependence of the average closed orbit radius $R = C/2\pi$ on the relative momentum, from 12 to 200 MeV. Markers are from one-turn raytracing. The solid line is from theory, for comparison, after Eq. 11.8 taken for $k = 7.6$ (Tab. 11.1) and reference momentum $p_{\mathrm{ref}} = 551.3$ MeV/c (150 MeV, radius $R_0 = 5.4$ m). They only differ by $\approx 1‰$

A gnuplot script can plot the scalloping $|R(\theta) - R|/R$. $R(\theta)$ is read from zgoubi.plt (column 10 therein) as in (b). The value of the average orbit radius $R = C/2\pi$ can be formulated using Eq. 11.11 with therein $p = qB\rho = q \times D \times BORO$, with D and BORO both read from zgoubi.plt (columns 2 and 40, respectively).

11.3

Zero-Chromaticity

(a) Momentum dependence of tunes.

MATRIX is used to compute the wave numbers, REBELOTE[K=0;IOPT=1] is used to repeat with a different momentum, the input data file is given in Tab. 20.70.

OBJET[KOBJ=5] defines a set of 13 particles with proper initial coordinate sampling for matrix computation, by MATRIX. Prior to matrix computation, the momentum-dependent closed orbit is found by FIT. REBELOTE changes the relative momentum D in OBJET, and repeats the sequence. The command MATRIX[PRINT] logs the transport coefficients to zgoubi.MATRIX.out, together with the beam matrix and tunes which are obtained from the hypothesis of periodicity

Table 20.70 Simulation input data file: compute the first order transport matrix of the DFD cell, for a series of momenta. Prior to matrix computation, the closed orbit is found by FIT. The INCLUDE grabs the dipole triplet segment of Tab. 20.68

```
Scan transport matrix of 150 MeV FFAG dipole triplet
'MARKER'  SFFAGZroChro_S                                                ! Just for edition purposes.
 'OBJET'
1839.090113                                                    !  Reference rigidity (150MeV proton).
5                                                                  ! Option for MATRIX computation.
.01 .001 .01 .001 0. 0.0001                                ! 13-trajectory sampling for MATRIX computation.
445.234   0.   0.  0. 0.   0.273042677097  'o'             ! Reference trajectory (number 1 in the 11-set).
1

'INCLUDE'                                                    ! Include the 30 degree sector dipole triplet,
1                                                                          ! within dedicated  LABEL1s.
./SFFAGCell.inc[#S_SFFAG150Cell:#E_SFFAG150Cell]

 'FIT'
1  noFinal
2 30 0  2.
2  1e-8 79                                                 ! A penalty value controls the accuracy
3.1 1 2 #End 0. 1. 0                          ! of the convergence of the constraints to the target values.
3.1 1 3 #End 0. 1. 0                                       ! 3.1 is the constraint for periodicity.

'MATRIX'
1 11  PRINT                              ! PRINT causes log of transport coefficients to zgoubi.MATRIX.out.

'REBELOTE'                                                          ! Repeat the previous sequence,
20 0 0  1                                                    ! 20 times; prior to repeating, change
1                                                         ! 1 parameter: parameter 35 under OBJET, namely,
OBJET 35 0.27304263798:1.              ! the relative momentum, D=p/p_ref, in the range 0.27304263798:1.

'SYSTEM'
1
gnuplot <./gnuplot_tunes.gnu                       ! Call  gnuplot script once that tracking is completed.

'MARKER'  SFFAGZroChro_E                                                ! Just for edition purposes.
 'END'
```

gnuplot script gnuplot_tunes.gnu, for Fig. 20.88:

```
# gnuplot_tunes.gnu
set xlabel "relative momentum p/p_{ref}"; set ylabel "{/Symbol n}_R,  {/Symbol n}_Z"; set y2label "penalty"
set xtics; set ytics nomirror; set y2tics nomirror; set key t l; set key maxrow 2; set logscale y2
# A system command to extract penalty values from zgoubi.res
system "grep 'Fit reached penalty value ' zgoubi.res | cat > grep.out"
k=7.6 ; Ncell = 12; set yrange [:4.5]; set y2range [1e-12:1e-4]
plot "zgoubi.MATRIX.out" u (0+$47):(Ncell* $56) w  p  pt 6 ps .9 tit "{/Symbol}_R", \
"zgoubi.MATRIX.out" u (0+$47):(Ncell* $57) w  p  pt 7 ps .9 tit "{/Symbol}_Z",  \
(x<1.03 ? sqrt(1+k) :1/0) w l lw 2 tit "\sqrt{(1+k)}" ,  "grep.out" u :5 axes x2y2
```

(MATRIX[IFOC=11]), namely by identifying [1, Sect. 6.5.6]

$$[T_{ij}] = I \cos\mu + J \sin\mu$$

Outcomes are plotted in Fig. 20.88. The radial tune ν_R is constant as expected from the zero-chromaticity resulting from the scaling law (momentum-independent index, Eq. 11.3). Such is not the case for the axial tune, ν_Z, this is due to the first order effect of fringe field extent on the axial focusing (see Sect. 18.3.1): fringe extent varies with orbit radius in correlation with gap height in the "gap shaping" hypothesis (Eq. 11.6; smaller gap at greater radius/greater energy).

(b) Momentum-dependent axial tune.

The variation of the axial tune with momentum, as observed in (a), is due to the fringe field extent decreasing with radius, following in that the gap height which induces the scaling field law $B(R) \propto R^k$ (Eq. 11.5): as a matter of fact the gap shape index value in the present radial sector model is $\kappa = 3$ (Tab. 20.68), resulting in a

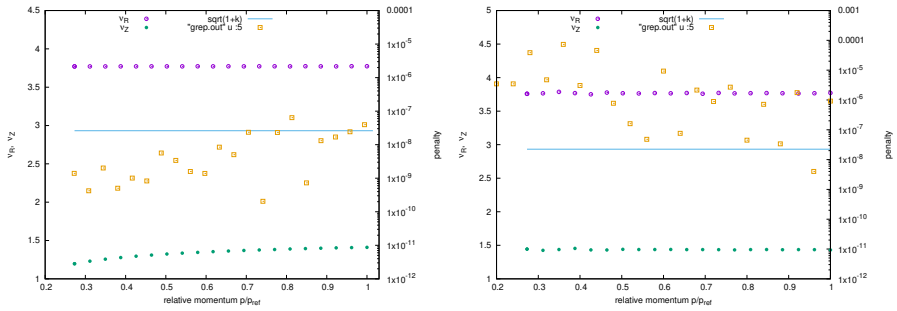

Fig. 20.88 Radial (ν_R) and axial (ν_Z) tunes (left vertical scale) of the 12-cell ring, as a function of relative momentum ($p/p_{\rm ref} = 1$ for 150 MeV). The penalty values (scattered squares, right vertical scale) monitor the FIT runs: a small penalty indicates convergence of FIT. Left: case of decreasing gap height with radius (equivalent to a decreasing fringe extent): $g(R) = g_0 \left(\frac{R_0}{R}\right)^3$. Right: case of linear increase of gap height with radius (equivalent to a linear increase of fringe extent): $g(R) = g_0 \left(\frac{R}{R_0}\right)$.

gap height (Eq. 20.68)

$$g(R) = g_0 \left(\frac{R_0}{R}\right)^3$$

The axial tune can be made constant using instead a gap law (Eq. 11.6)

$$g(R) = g_0 \left(\frac{R}{R_0}\right) \qquad (\kappa = -1)$$

i.e., gap height proportional to momentum/R [2, 3]. The simulation is obtained by changing the lines of concern under FFAG keyword (Tab. 20.68), namely

change “6.3 3. ! EFB [etc.]” to “6.3 − 1. ! EFB [etc.]”

at the 6 EFBs. The resulting tunes are displayed in Fig. 20.88: ν_R is marginally affected, whereas ν_Z is now about constant.

A FIT procedure can be further attempted, in order to try and improve things, proceeding in the following way:

- vary κ
- constrain ν_Z =constant at a few energies in the 12-150 MeV range.

However, as expected from theory, it is found that the constraint is already fairly satisfied with $\kappa = -1$.

(d) Momentum compaction and transition γ_{tr}

TWISS keyword is used to compute various first and second order optical parameters - it does a little more than MATRIX, and similarly uses the 13-particle

OBJET[KOBJ=5]. A typical input file including TWISS is given in Tab. 20.71. Results are given in Tab. 20.72.

It is expected for the momentum compaction to satisfy $\alpha = \frac{\Delta C}{C} / \frac{\Delta p}{p} = 1/(1 + k)$ (Eq. 11.17). In the present design $k = 7.6$ in all three dipoles of the triplet (Tab. 20.68), yielding $\alpha = 0.11628$. This approximation appears valid at high energy where $\alpha = 0.11620$ (Tab. 20.71), however it is not the case at low energy where the numerical integration yields $\alpha = 0.42528$. This discrepancy is attributed to the strong departure of the azimuthal variation of the field at 12 MeV, $B(\theta)|_{12\,\mathrm{MeV}}$ (Fig. 20.84), from a hard edge model which leads to Eq. 11.17.

Table 20.71 Simulation input data file: TWISS command, to obtain beam matrix, momentum compaction, chromaticities, etc. The initial reference coordinates, under OBJET, are for 12 MeV; reference coordinates for 150 MeV (to substitute to the previous ones) have been added as a comment. TWISS proceeds in 3 stages: it first computes tunes of an on-momentum particle, then for $\pm\delta p/p$ off-momentum particles; at each stage, FIT ensures that the reference particle (1st particle of the 11-set) is on the closed orbit

```
Compute momentum compaction.
'MARKER' SFFAG_TWISS_S
 'OBJET'
1839.090113                                                    !  Reference rigidity (150MeV proton).
5                                                                 ! Option for MATRIX computation.
.01 .001 .01 .001 0. 0.0001                                ! 13-trajectory sampling for TWISS computation.
445.234 0. 0. 0. 0. 0.273042677097  'o'     ! 12 MeV reference trajectory (traj. number 1 in the 11-set).
1

! 150 MeV reference trajectory, should replace the 12 MeV data line above:
! 517.4981  0.   0.  0. 0.   1.  'o'

'INCLUDE'                                                  ! Include the 30 degree sector dipole triplet,
1                                                                    ! within dedicated  LABEL1s.
./SFFAGCell.inc[#S_SFFAG150Cell:#E_SFFAG150Cell]
'FIT'
1  noFinal
1 30 0  2.
2  1e-8 79    ! A penalty value controls accuracy of convergence of the constraints to the target values.
3.1 1 2 #End 0. 1. 0      ! 3.1 is the constraint for periodicity; coordinate 2 (Y) of particle 1, here;,
3.1 1 3 #End 0. 1. 0                                          ! coordinate 3 (T) of particle 1, here;.
'TWISS'
2 1. 1.
'MARKER' SFFAG_TWISS_E
'END'
```

Table 20.72 Outcomes of TWISS computation out of zgoubi.res listing, including beam matrix, tunes, momentum compaction, chromaticities

Case of 12 *MeV optics*:

```
Reference, before change of frame (particle #  1  - D-1,Y,T,Z,s,time)  :
-7.26957323E-01   4.45233802E+02   6.40323244E-05   0.00000000E+00   0.00000000E+00   2.41165083E+02   5.07793867E-02

Reference, after change of frame (particle #  1  - D-1,Y,T,Z,s,time)  :
-7.26957323E-01   0.00000000E+00   0.00000000E+00   0.00000000E+00   0.00000000E+00   2.41165083E+02   5.07793867E-02

Beam  matrix  (beta/-alpha/-alpha/gamma) and  periodic  dispersion  (MKSA units)
         0.734624     0.000003     0.000000     0.000000     0.000000     0.514568
         0.000003     1.361240     0.000000     0.000000     0.000000    -0.000000
         0.000000     0.000000     4.398783    -0.000040     0.000000    -0.000000
         0.000000     0.000000    -0.000040     0.227336     0.000000     0.000000

                         Betatron  tunes  (Q1 Q2 modes)
                NU_Y =  0.31422833         NU_Z =  0.99804552E-01

                         Momentum compaction :
                      dL/L / dp/p =  0.42528937

                         Transition gamma  =  1.53340804E+00

                         Chromaticities :
                dNu_y / dp/p =  1.92734237E-04              dNu_z / dp/p =  2.19919557E-02
```

Case of 150 *MeV optics*:

```
Reference, before change of frame (particle #  1  - D-1,Y,T,Z,s,time)  :
 0.00000000E+00   5.17498491E+02  -2.99045520E-05   0.00000000E+00   0.00000000E+00   2.80426451E+02   1.84634162E-02

Reference, after change of frame (particle #  1  - D-1,Y,T,Z,s,time)  :
 0.00000000E+00   0.00000000E+00   0.00000000E+00   0.00000000E+00   0.00000000E+00   2.80426451E+02   1.84634162E-02

Beam  matrix  (beta/-alpha/-alpha/gamma) and  periodic  dispersion  (MKSA units)
         0.853519    -0.000046     0.000000     0.000000     0.000000     0.600422
        -0.000046     1.171620     0.000000     0.000000     0.000000    -0.000009
         0.000000     0.000000     4.322948     0.000012     0.000000    -0.000000
         0.000000     0.000000     0.000012     0.231324     0.000000     0.000000

                         Betatron  tunes  (Q1 Q2 modes)
                NU_Y =  0.31448874         NU_Z =  0.11757537

                         Momentum compaction :
                      dL/L / dp/p =  0.11619673

                         Transition gamma  =  2.93361449E+00

                         Chromaticities :
                dNu_y / dp/p = -5.78695533E-04              dNu_z / dp/p =  4.78678315E-03
```

11.4 Beam Envelopes; Phase Space

(a) Motion envelopes.

There is various possibilities to get the beam envelopes along the cell. One consists in raytracing a few particles with initial coordinates taken on an ellipse. Another method tracks a single particle, for a few tens of turns. A third posibility consists in pushing the initial beam matrix $\sigma(s_0)$ through the cell, using $\sigma(s) = T(s \leftarrow s_0)\sigma(s_0)\tilde{T}(s \leftarrow s_0)$, by computing $T(s \leftarrow s_0)$ from the stepwise particle coordinates in the option OBJET[KOBJ=5] [7].

In any case, linear envelopes, with maximal excursion $\sqrt{(\frac{\varepsilon_Y}{\pi}\beta_Y(s))}$ and $\sqrt{(\frac{\varepsilon_Z}{\pi}\beta_Z(s))}$, require paraxial motion.

The first method is retained, here. Set IL=2 under FFAG to have particle data logged, step by step, in zgoubi.plt. Graphs of the trajectories of the beam bundle across the cell, at 12 and 150 MeV are given in Fig. 20.89.

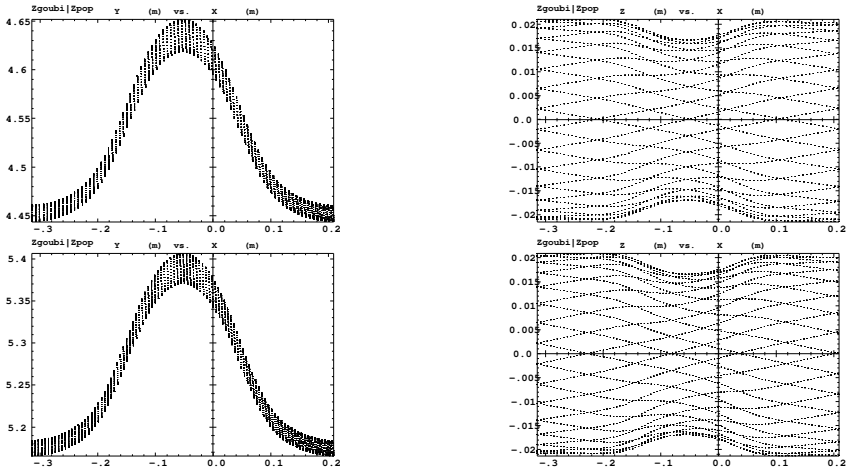

Fig. 20.89 Radial (left) and axial (right) beam bundle trajectories across the FFAG triplet cell; top row: 12 MeV, bottom row: 150 MeV. Graphs obtained using zpop, which reads particle data from zgoubi.plt (menu 7; 1/1 to open zgoubi.plt; 2/[8,2] to select Y (radius) versus X (azimuthal angle) [or 2/[8,4] to select Z (axial coordinate)]; 7 to plot)

.

Particle trajectories result from initial coordinates taken on a small invariant value (an ellipse), in both radial and axial planes, namely, $\varepsilon_Y/\pi = \varepsilon_Z/\pi = 0.1$ mm (Tab. 20.73). The definition of the initial coordinates on an ellipse uses the keyword

Table 20.73 Simulation input data file: proper OBJET, using KOBJ=8, to define a beam bundle by initial reference orbit coordinates, and Courant invariant values

Case of 12 *MeV optics*:

```
 'OBJET'
1839.090113                                                  !  Reference rigidity (150MeV proton).
8                                                             ! Option for particles on an ellipse.
30 30 1                                  ! 30 particle evenly spaced on Y-T ellipse, same on Z-P ellipse.
4.45234 0. 0. 0. 0. 0.273042677097 'o'          ! Reference trajectory (note the units: units: m, rad).
0. 0.734624 1e-4                                              ! alpha_Y, beta_Y, invariant value.
0. 4.399057 1e-4                                              ! alpha_Z, beta_Z, invariant value.
0. 1. 0.                                                      ! alpha_X, beta_X, invariant value.
```

Case of 150 *MeV optics*:

```
 'OBJET'
1839.090113                                                  !  Reference rigidity (150MeV proton).
8                                                             ! Option for particles on an ellipse.
30 30 1                                  ! 30 particle evenly spaced on Y-T ellipse, same on Z-P ellipse.
517.4981 0. 0. 0. 0. 1. 'o'                     ! Reference trajectory (note the units: units: m, rad).
0. 0.853818 1e-4                                              ! alpha_Y, beta_Y, invariant value.
0. 4.323902 1e-4                                              ! alpha_Z, beta_Z, invariant value.
0. 1. 0.                                                      ! alpha_X, beta_X, invariant value.
```

OBJET[KOBJ=8]. The ellipse parameters, $\alpha_{Y,Z}$, $\beta_{Y,Z}$, are taken from outcomes of the previous exercise (Tab. 20.72).

Note that the rather large initial invariant values (0.1πmm) result in the two motions to be slightly coupled (in the presence of non-zero axial motion), the initial elliptical invariant is not preserved during the propagation, see next question.

(b) Multiturn tracking, phase space.

The definition of the initial coordinates of the particle to be tracked uses the keyword OBJET[KOBJ=8] as in the previous method. However, considering the input data in Tab. 20.73,

$$change \quad \text{“30 30 1”} \qquad to \qquad \text{“1 1 1”}$$

Multiturn tracking reveals that 0.1 mm motion invariants are large enough that (i) they are distorted by field non-linearities (compared to ellipses in the case of paraxial motion), and (ii) Y and Z motions feature non-linear coupling. This shows in Fig. 20.90 which displays phase space motion in the two cases of initial coordinates taken on an $\varepsilon_Y/\pi = \varepsilon_Z/\pi = 0.1$ mm ellipse and on an $\varepsilon_Y/\pi = \varepsilon_Z/\pi = 1\ \mu$m ellipse. In the first case the motion is not elliptical, whereas in the second case, much closer to paraxial conditions, the phase space portrait is an ellipse, with no visible coupling (a thin ellipse, in both planes).

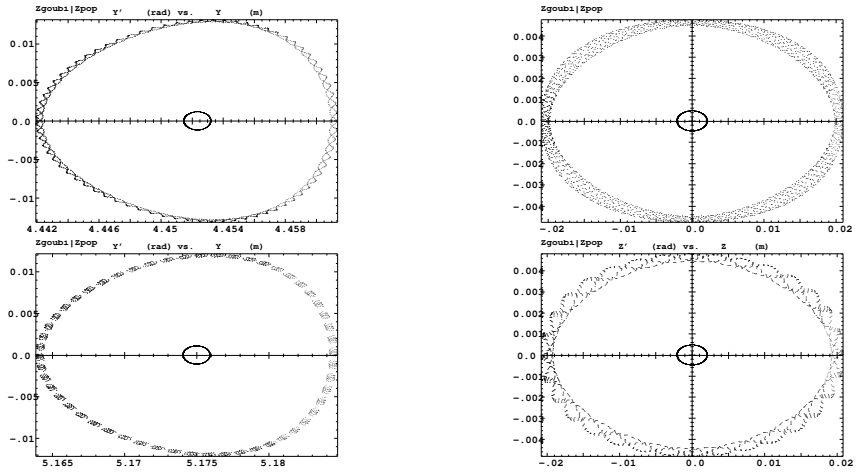

Fig. 20.90 Multiturn tracking: radial (left) and axial (right) phase space motion, observed at the end (middle of the drift) of an FFAG triplet cell; top row: 12 MeV, bottom row: 150 MeV. The central quasi-elliptical motion is for $\varepsilon_Y/\pi = \varepsilon_Z/\pi = 1\ \mu$m, the outer motion, distorted and coupled, is for $\varepsilon_Y/\pi = \varepsilon_Z/\pi = 0.1$ mm. Graphs obtained using zpop, which reads particle data from zgoubi.fai (menu 7; 1/5 to open zgoubi.fai; 2/[2,3] to select T versus Y (or, 2/[4,5] to select P versus Z); 7 to plot)

11.5

Acceleration: Transverse Betatron Damping

(a) Acceleration cycle in RACCAM ring.

A typical prior check: it is a good idea to first validate the input data file to be used for acceleration, by producing and checking a few closed orbits, or one-turn beam matrices. An input data file in that aim is given in Tab. 20.74. Excerpts from zgoubi.res so obtained are given in Tab. 20.75, they show periodic orbits at expected radii, respectively $Y_0 = 440.5\,\text{cm}$ (10 MeV) and $Y_0 = 526.9\,\text{cm}$ (200 MeV), and expected beam matrices (compare to Tab. 20.72).

Following these satisfactory preliminary checks, an input data file set for acceleration from 10 to 200 MeV is derived, Table 20.76. Note the "12 *" under INCLUDE, for 12 cells. The cell, a dipole triplet with half-drifts on both sides, is as in Tab. 20.68 except for three parameters:

(i) IL has been set to 0, to inhibit output to zgoubi.plt as this save on computing time,

(ii) the integration step size has been set to $\Delta s = 1\,\text{cm}$, for accuracy over the many turn acceleration cycle.

(iii) FFAG allows a few methods for the numerical integration, KIRD=0 was used in Tab. 20.68, whereas the method retained here instead, for a change (an interesting exercise would consist in comparing the outcomes from the two methods), is KIRD=2; as a consequence

"0 2 ! *Field computation analytic 2nd order (take KIRD = 2, 25 or 4 for flying grid etc."*

in Tab. 20.68, is changed to (comments, beyond the exclamation mark, have no effect!)

"2 10. ! *Field computation method : 3 * 3 flying grid, 2nd degree interpolation."*

The consequence is that the field and derivatives [1, Sect. 1.2, 1.2.1] are computed using a small 3×3 node flying grid technique (that is what '2' stands for, '10' stands for the grid mesh size, taken equal to $\Delta s/10$), whereas in the previous exercises, given KIRD=0, field and derivatives are computed from (hard-coded) analytical expressions [1, Part B, FFAG] [4].

Setting up the acceleration, now:

- PARTICUL[PROTON] is necessary as CAVITE is used: it allows converting energy change in rigidity change (zgoubi pushes particles using rigidity),

- SCALING, akin to a "power supply rack", provides the RF program to CAVITE, by reading it from the ancillary file zgoubi.freqLaw.In, see below,

- CAVITE boosts the particle(s) at each pass, following a pre-defined RF program,

- REBELOTE sends the execution pointer back to the top of the input data file, for multiturn tracking. The number of turns results from a peak voltage $\hat{V} = 40\,\text{kV}$ and synchronous phase 20° (Tab. 20.76), the 10 to 200 MeV acceleration range is covered in $(200 - 10) \times 10^3/[40 \times \sin(20°)] \approx 13900$ turns.

For simplicity the RF program is limited in the present case to the turn dependence of RF frequency (peak voltage and synchronous phase maintained constant). Elaborating zgoubi.freqLaw.In (essentially two columns: RF frequency versus turn number) requires the following steps:

(i) run a search for closed orbits for a few tens of energies in the range 10 to 200 MeV. The corresponding data file is given in Tab. 20.77. Time of flight, derived from

path length and particle velocity, is part of the outcome of orbit computation as PARTICUL provides necessary particle data in that aim. That yields the turn dependence of RF frequency, namely, $f_{\mathrm{RF}} = h \times f_{\mathrm{rev}} = v/C$ (h=1, here). Note that in the absence of orbit defects or other tailored bumps, the frequency law may be obtained, more simply, from the theoretical orbit length $C(p) = C_0(p/p_0)^{\frac{1}{k+1}}$ (Eq. **??**), as it is expected to yield similar values to the aforementioned closed orbit raytracing;

(ii) store these turn-frequency data, properly formatted, in zgoubi.freqLaw.In (Tab. 20.78). zgoubi.freqLaw.In does not need to contain all turns, zgoubi will interpolate from the set of values found therein.

Table 20.74 Simulation input data file: checking the file set up for acceleration. This data file is derived from the acceleration input file in Tab. 20.76, and provides periodic matrix computation at 10 MeV and 200 MeV, combining OBJET[KOBJ=5] (to allow computation by MATRIX), FIT (find the orbit) and REBELOTE (repeat for an additional momentum)

```
Check inut data prior to acceleration cycle
'OBJET'
1839.090113 150MeV
5
.001 .01 .001 .01 .001 .0001
440.54197   0.   0.000  0. 0.  0.2491207073   'o'                          ! 10MeV proton, Brho=458.155.
'PARTICUL'
PROTON
'INCLUDE'                                                 ! Include the 30 degree sector dipole triplet,
1                                                                ! within dedicated  LABEL1s.
./SFFAGCell.inc[#S_SFFAG150Cell:#E_SFFAG150Cell]
 'FIT2'
1  nofinal
1 30 0  2.
1  1e-9 99          ! A penalty value controls the accuracy of the convergence to periodic coordinates.
3.1 1 2 #End 0. 1. 0                                          ! 3.1 is the constraint for periodicity.
'FAISCEAU'                                                ! Log particle coordintes in zgoubi.res, here.
'MATRIX'                                                                  ! Periodic matrix.
1 11
'REBELOTE'
1 0 0  1                                                                  ! Repeat just once;
1                                ! prior to repeat, change parameter 35 under OBJET, which is D=p/p_ref,
OBJET 35 1.1688582876:1.1688582876                                ! to the value D=1.1688582876.
'END'
```

(b) Transverse motion.

The acceleration simulation file is that of Tab. 20.76. Longitudinal and transverse motion samples are displayed in Figure 20.91. The integration step size is Δs = 1 cm in these simulations. Taking KIRD=0 instead (see remarks above), all the rest unchanged, results in marginal difference.

(c) Track a particle bunch.

Use MCOBJET[KOBJ=3] here, to populate an initial Gaussian distribution with random transverse coordinates. The periodic optical functions needed in MCOBJET are taken from the 10 MeV beam matrix in Tab. 20.75, namely, $\alpha_x = \alpha_y = 0$, $\beta_x = 0.7268$ m, $\beta_x = 4.4988$ m. This yields

```
'MCOBJET'
1839.08991465                                                             !  150MeV proton.
3
200                                                                       ! 200 particles.
2 2 2 2 1 1                                           ! Gaussian radial and axial distributions.
4.4054197   0.   0.000  0. 0. 0.24912070392                                ! 10MeV closed orbit.
0.  0.7268  1e-8 3                                     ! alpha_Y, beta_Y, epsilon_Y/pi, cut-off.
0.  4.4988  1e-8 3                                     ! alpha_Z, beta_Z, epsilon_Z/pi, cut-off.
0.  1.      0.   3                                     ! alpha_X, beta_X, epsilon_X/pi, cut-off.
```

Table 20.75 Output file: checking the file set up for acceleration. This table shows excerpts from zgoubi.res, following from the input data file in Tab. 20.74, namely, the closed orbit, matrix and tunes for 10 MeV (relative momentum D=0.2491, top part) and for 200 MeV (D=1.1689, bottom part). Particle 1 is the reference particle for the computation of the transport matrix from which the beam matrix is deduced

```
************************************************************************************************************************
                                        TRACE DU FAISCEAU
                                    (follows element #      6)
                                        13 TRAJECTOIRES
                                OBJET                                                   FAISCEAU
        D      Y(cm)     T(mr)     Z(cm)     P(mr)      S(cm)      D-1     Y(cm)    T(mr)    Z(cm)    P(mr)      S(cm)
0  1  0.2491  440.542   0.000     0.000     0.000      0.0000   -0.7509  440.542   0.000    0.000    0.000    2.386113E+02
                Time of flight (mus) :  5.49502499E-02 mass (MeV/c2) :   938.272

      Beam  matrix  (beta/-alpha/-alpha/gamma) and  periodic  dispersion  (MKSA units)
          0.726851     0.000000     0.000000     0.000000     0.000000     0.508871
          0.000000     1.375798     0.000000     0.000000     0.000000    -0.000000
          0.000000     0.000000     4.498812    -0.000001     0.000000     0.000000
          0.000000     0.000000    -0.000001     0.222281     0.000000     0.000000

                                Betatron  tunes
                    NU_Y =  0.31421037         NU_Z =  0.96625558E-01
************************************************************************************************************************
                                        TRACE DU FAISCEAU
                                    (follows element #      6)
                                        13 TRAJECTOIRES
                                OBJET                                                   FAISCEAU
        D      Y(cm)     T(mr)     Z(cm)     P(mr)      S(cm)      D-1     Y(cm)    T(mr)    Z(cm)    P(mr)      S(cm)
0  1  1.1689  526.956   0.000     0.000     0.000      0.0000    0.1689  526.956  -0.000    0.000    0.000    2.855586E+02
                Time of flight (mus) :  1.68242271E-02 mass (MeV/c2) :   938.272

      Beam  matrix  (beta/-alpha/-alpha/gamma) and  periodic  dispersion  (MKSA units)
          0.869721    -0.000000     0.000000     0.000000     0.000000     0.611749
         -0.000000     1.149794     0.000000     0.000000     0.000000    -0.000000
          0.000000     0.000000     4.384709    -0.000001     0.000000     0.000000
          0.000000     0.000000    -0.000001     0.228065     0.000000     0.000000

                                Betatron  tunes
                    NU_Y =  0.31439931         NU_Z =  0.11802584
************************************************************************************************************************
```

7294 to substitute to OBJET in Tab. 20.76.

Table 20.76 Simulation input data file: proton acceleration from 10 MeV to about 200 MeV, in 13901 turns around the 12-cell ring. Note: the step size must be in the centimeter range for multiturn accuracy, in such non-linear field (substitute "1." (cm) to "3.0079078598", in the INCLUDE file SFFAGCell.inc, Tab. 20.68)

```
Acceleration from 10 to 150 MeV.
'MARKER'  SFFAGParoAccel_S                                          ! Just for edition purposes.
'OBJET'
1839.08991465                                                                ! 150MeV proton.
2
1  1
440.54197 3. 0. 1. 0. 0.24912070392  'o'            ! 10MeV proton,  Brho=1839.090113 * 0.2491207073.
1                                              ! Y_0 is +2 cm wrt. closed orbit R=445.234; Z_0=1 cm.
'PARTICUL'                                  ! Particle data will allow compute energy, time of flight.
PROTON                                                ! Acceleration requires particle data.
'SCALING'                                               ! SCALING is used to control CAVITE.
 1   1
CAVITE
 -2        ! Option -2 causes
  1   !  unused with option -2
  1   !  unused  with option -2
'PICKUPS'
 1
 #E
'FAISTORE'
zgoubi.fai AftCAV          ! (use "b_" for binary storage: b_zgoubi.fai). Storage is at LABEL1=AftCAV.
 1
'INCLUDE'                                          ! Include the 30 degree sector dipole triplet,
1                                                                ! within dedicated  LABEL1s.
12 * SFFAGCell.inc[#S_SFFAG150Cell:#E_SFFAG150Cell]           ! Build the ring from 12 cell INCLUDEs.
'CAVITE'
6          ! Option 6 allows reading RF program from an exeternal file (default is zgoubi.freqLaw.In).
0.  10.                                                ! unused; kinetic energy at start (MeV).
40000.  0.349066                                 ! Peak voltage; synchronous phase (rad), 20 degree.
'FAISCEAU'                                           ! Log particle coordintes in zgoubi.res, here.
'MARKER' AftCAV                                            ! Storage by FAISTORE is effective here.
'REBELOTE'                                    ! Repeat sequence 12999 times. Log count to video every
13900 0.2 99                                ! other 10 turns. '99': ignore OBJET at subsequent passes.
'MARKER'  SFFAGParoAccel_E                                          ! Just for edition purposes.
'END'
```

Table 20.77 Simulation input data file: search closed orbits for a few tens of energies in the range 10 to 200 MeV

```
FFAG triplet. 150MeV machine. Find orbits from 10 to 200 MeV.
'OBJET'
1839.08991465                                                                !  150MeV proton.
2
1 1
440.54197   0.   0.000  0. 0.  0.2491207073   'o'                          ! 10MeV proton, Brho=458.155.
1
'PARTICUL'
PROTON
'INCLUDE'                                          ! Include the 30 degree sector dipole triplet,
1                                                                ! within dedicated  LABEL1s.
SFFAGCell.inc[#S_SFFAG150Cell:#E_SFFAG150Cell]                 ! INCLUDE the FFAG triplet sector.
'FIT'                                           ! Find initial coordinate uch that final = initial.
1
1 30 0 1.
1
3.1 1 2 #End 0. 1. 0
'FAISTORE'
RFprogram_orbits.In
1
'REBELOTE'                                               ! Repeat 50 times, from 10 to 200 MeV.
50 0.2 0 1
1
OBJET  35  0.24912070392:1.16885844252            ! Change relative momentum value, from 10 to 200MeV.
'END'
```

Table 20.78 Top and bottom parts of the RF program file zgoubi.freqLaw.In, as read by zgoubi when using CAVITE[IOPT=6]. Zgoubi actually only requires turn number, column 1, and revolution time which is computed from the cumulated time-of-flight across the cells, column 4. The other four columns are unused subproducts of the calculations performed by the RF program from the turn-by-turn closed orbit data

turn#	cell Time of flight, tauCell	cumulated phase phi	cumulated time of flight, oclock	kinetic energy, Ekin	Test. Expected one
1.0000E+00	5.49502566E-02	0.0000E+00	6.59403079E-01	1.0000E+01	1.0000E+00
2.0000E+00	5.49185204E-02	6.28318531E+00	1.31844010E+00	1.00136808E+01	9.99962422E-01
3.0000E+00	5.48868211E-02	1.25663706E+01	1.97711108E+00	1.00273616E+01	9.99925969E-01
4.0000E+00	5.48551589E-02	1.88495559E+01	2.63541601E+00	1.00410424E+01	9.99890628E-01
5.0000E+00	5.48235338E-02	2.51327412E+01	3.29335493E+00	1.00547232E+01	9.99856388E-01
6.0000E+00	5.47919462E-02	3.14159265E+01	3.95092786E+00	1.00684040E+01	9.99823237E-01
7.0000E+00	5.47603962E-02	3.76991118E+01	4.60813483E+00	1.00820848E+01	9.99791162E-01
8.0000E+00	5.47288840E-02	4.39822972E+01	5.26497589E+00	1.00957656E+01	9.99760153E-01
.....					
1.3881E+04	1.67887669E-02	8.72106121E+04	3.95518038E+03	1.99889584E+02	1.00389444E+00
1.3882E+04	1.67931495E-02	8.72168952E+04	3.95538164E+03	1.99903264E+02	1.00342779E+00
1.3883E+04	1.67975355E-02	8.72231784E+04	3.95558299E+03	1.99916945E+02	1.00296144E+00
1.3884E+04	1.68019247E-02	8.72294616E+04	3.95578442E+03	1.99930626E+02	1.00249542E+00
1.3885E+04	1.68063170E-02	8.72357448E+04	3.95598595E+03	1.99944307E+02	1.00202973E+00
1.3886E+04	1.68107123E-02	8.72420280E+04	3.95618757E+03	1.99957988E+02	1.00156440E+00
1.3887E+04	1.68151104E-02	8.72483112E+04	3.95638927E+03	1.99971668E+02	1.00109943E+00
1.3888E+04	1.68195111E-02	8.72545944E+04	3.95659107E+03	1.99985349E+02	1.00063485E+00
1.3889E+04	1.68239142E-02	8.72608775E+04	3.95679295E+03	1.99999030E+02	1.00017066E+00

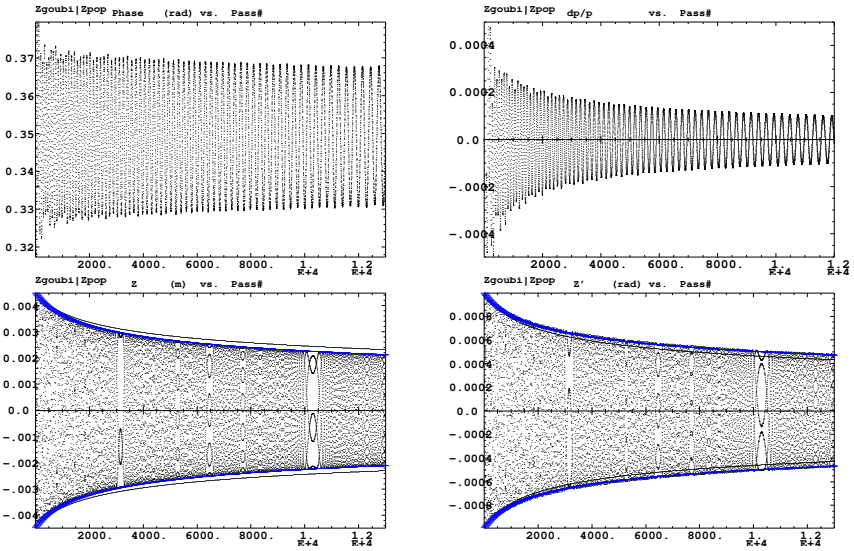

Fig. 20.91 An acceleration from 10 to 200 MeV. Top row: RF phase (left) and relative momentum (right) as a function of turn number, over an acceleration cycle. Bottom row: axial excursion (left) and angle (right). Dots are turn-by-turn particle coordinates from numerical tracking. The theoretical envelops (bottom plots, thick blue curves) are from Eqs. 11.21. The thin curves show what the envelop would be in the case of a mere $1/\sqrt{\beta\gamma}$ damping (which is the case if the closed orit is fixed, as in a betatron, or in a pulsed synchrotron)

20.6.2 RACCAM Proton Therapy Spiral Sector FFAG

This series of exercises concerns the 180 MeV spiral sector proton therapy FFAG design displayed in Fig. 11.8, and its simulation using FFAG-SPI. The design parameters of the ring and of its cell dipole are given in Tab. 11.2 [2, 3, 5, 6]. The cell geometry is sketched in Fig. 20.92, orbits through a pair of cells are sketched in Fig. 20.93 as an illustration. Note the presence of field clamps on both sides of the dipole, these can be simulated in FFAG-SPI, by adding narrow, negative field spiral sectors adjacent to the main dipole [5].

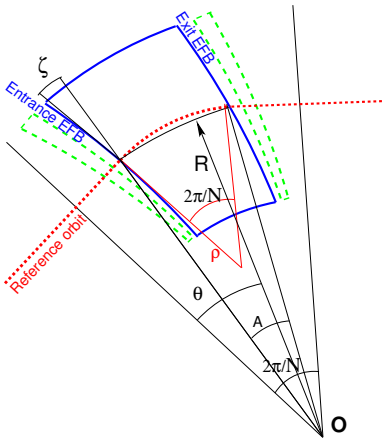

Fig. 20.92 A sketch of RACCAM spiral sector dipole and $2\pi/10$ cell. O is the center of the ring and the EFBs form a sector angle A. Note that the reference orbit is not strictly circular, the bending radius is not constant along the trajectory over the $2\pi/N$ arc (a line of constant field is an R-radius arc, centered on O). Field clamps can be seen represented (dashed lines), on both sides of the dipole

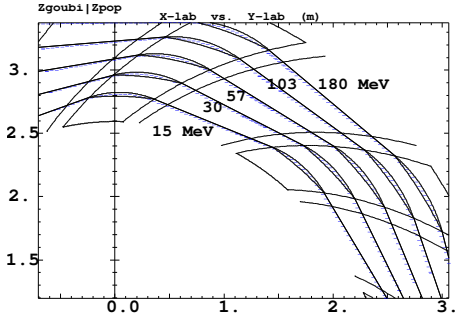

Fig. 20.93 A simulation of a pair of cells of RACCAM FFAG ring in zgoubi, including a few orbits, using the keyword FFAG-SPI. The simulation includes field clamps on both sides of the dipoles

11.6

Field in a Spiral Sector Dipole

The mid-plane magnetic field can be generated from Eq. 11.14, with geometrical and field data taken from Tab. 11.2. This is the FFAG-SPI field model, used here to produce the field along trajectories. It is based on the field modeling technique described in Sect. 11.2.2. The input data file is given and commented in Tab. 20.79, which can be referred to for details.

The mid-plane field data $B_Z(R,\theta)|_{Z=0}$ are arranged under the form of a 2D even meshing, this is in order to allow possible further use, with TOSCA or POLARMES keywords. In order to generate a field map, from particle raytracing, a set of 29 trajectories is launched, with initial coordinates $Y_0,\ T_0,\ Z_0,\ P_0$ and relative momentum $D = p/p_{\text{ref}}$ defined using OBJET[KOBJ=1]: they all have initial incidence $T_0 = 0$, normal to the $AT = 45.83662°$ angular sector which contains the magnet, whereas initial radii Y_0 are evenly spaced over the useful field region, namely

$$Y_0 : r_1 \rightarrow r_{29},\ \text{step}\ \Delta r \qquad \text{with}\ r_1 = 282\,\text{cm},\ r_{29} = 340\,\text{cm},\ \Delta r = 1\,\text{cm}$$

Axial motion is taken null, $Z_0 = 0$ and $P_0 = 0$. For each particle, the motion is forced to maintain constant radius, $r \in \{r_1, r_{29}\}$, throughout the dipole, using CONSTY. The integration step size is $\Delta s = 3.46\,\text{cm}$, resulting in 81 steps over

$$\theta : \theta_1 \rightarrow \theta_{81},\ \text{step}\ \Delta\theta = \Delta s/R_0, \qquad \text{with}\ \theta_1 = 0,\ \theta_{81} = AT,\ \Delta\theta = 0.572906°$$

with radius $R_0 = 346.031$ cm, and $AT = 45.83662°$ the sector opening. AT includes extra extent (thus, beyond the 36° angular extent of a period) in order to avoid cutting off field tails. In doing so, the angles TE and TS of FFAG-SPI's KPOS parameters, are used to re-establish the 36° periodicity. This generates the mid-plane field $B_Z(r,\theta)$ over a $N_r \times N_\theta = 29 \times 81$ node 2D meshing, displayed in Fig. 20.94. Note that if a 3D map is desired instead, a Z_0 sampling can be added in OBJET, as CONSTY also forces Z to its initial value Z_0.

Table 20.79 Simulation input data file: RACCAM 36 degree cell, comprised of a spiral sector dipole. The FFAG-SPI keyword allows defining up to 5 indepent dipoles in an AT angular sector; only one is defined in the present case, in order to generate field in a single dipole (note: field clamps could be simulated by adding two reversed-field narrow sectors on both sides of the main dipole). CONSTY option allows to generate a field map by raytracing a set of trajectories on *constant radius*, with *constant integration step size*. The present input data file is saved under the name RACCAMCell.inc, it also defines the sequence segment #S_RACCAMCell to #E_RACCAMCell, for use in INCLUDEs in subsequent exercises

```
RACCAMCell.inc file. 36 deg Spiral sector.
'MARKER'  RACCAMProbFieldMap_S
 'OBJET'
2029.47926                                                              ! Rigidity of 180 MeV proton.
1
29 1 1 1 1 1                      ! This creates 29 trajectories, corresponding to as many radial steps,
1. 0. 0. 0. 0. 0.                    ! whereas theta-steps result from the integration step size, below.
311.  0.  0.  0. 0.  1.          ! Yo is half-way between a minimum  282 cm   and       a maximum 340 cm.
                                          ! (injection region, 15MeV)  (extraction region, 180MeV)
'PARTICUL'                                                ! Allows computation of particle energy.
PROTON
'OPTIONS'
1 1
CONSTY ON                                ! Forces particles on Y=Yo and Z=Zo, in subsequent raytracing.

'MARKER'  #S_RACCAMCell
'FFAG-SPI'
0    ! Set IL=2 to store particle and field data along trajectories (in zgoubi.plt) for further plotting.
1  45.83662  346.031               ! Number of dipoles over AT; AT; R0. Bend angle is AT+TE-TS = 36 deg.
12 0.  17.   5.                                                 ! ACN, dR0, B0, geometrical index k.
8.95 -0.52    ! EFB 1 : lambda~gap size, kappa=gap shape index: detemines radius-dependent fringe extent.
6  .1455   2.2670  -.6395  1.1558  0. 0.  0.
6.120000E+00  5.370000E+01 1.E6  -1.E6  1.E6  1.E6                ! Entrance face azimuth; spiral angle.
8.95 -0.52    ! EFB 2 : lambda~gap size, kappa=gap shape index: detemines radius-dependent fringe extent.
6  .1455   2.2670  -.6395  1.1558  0. 0.  0.
-6.120000E+00  5.370000E+01 1.E6  -1.E6  1.E6 1.E6                   ! Exit face azimuth; spiral angle.
0. -1
0  0.   0.   0.   0.   0. 0.  0.
0.  0.   0.    0.    0. 0.
2  10.                           ! KIRD = 2: 3*3 flying grid interpolation, grid size is step size/Resol.
3.46                                                                    ! Step size (cm).
2
0. -0.295280245 0. -0.123598776                  ! RE, TE, RS, TS. Total deviation is AT+TE-TS = 36 deg.
'MARKER'  #E_RACCAMCell

'SYSTEM'3
2                                                          ! A 'call system' for next 2 commands:
gnuplot < ./gnuplot_Zplt_fieldMap.gnu                ! plot field data logged in / read from zgoubi.plt;
! okular gnuplot_Zplt_fieldMap.eps &                      ! view graph - requires a .eps viewer.

'MARKER'  RACCAMProbFieldMap_E
 'END'
```

---

gnuplot script gnuplot_Zplt_fieldMap.gnu, for Fig. 20.94:

```
#gnuplot_Zplt_fieldMap.gnu
set xlabel 'X [cm]' ; set ylabel 'Y [cm]' ; set zlabel 'B [kG]'
set xtics  340, 40, 420 ; set hidden3d ; set view 63, 94 ; set zrange[0:22]
splot "zgoubi.plt" u ($10*cos($22)):($10*sin($22)>-50? $10*sin($22) :1/0):($25) w p pt 5 ps .8 lc palette notit; pause 1
```

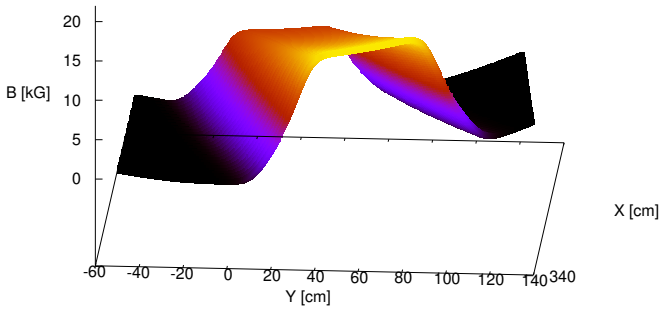

Fig. 20.94 Using FFAG-SPI theoretical modeling: mid-plane magnetic field in RACCAM spiral sector dipole, in the laboratory frame ($X = R\cos\theta$ and $Y = R\sin\theta$). The meshing geometry is obtained by ray-tracing 29 particles forced on circular trajectories evenly spaced in radius with constant angular integration step size. FFAG-SPI uses the spiral sector analytical field model of Eq. 11.14

11.7

Orbits, Scalloping

(a) Periodic orbits.

The input data file in Tab. 20.80 will produce 10 closed orbits (found one by one by FIT) for as many different momenta (REBELOTE repeats the sequence) ranging in (relative to $p_{\mathrm{ref}} = 608.422\,\mathrm{MeV/c}$, 180 MeV proton) $p/p_{\mathrm{ref}} = 0.2768526 : 1$ (15 to 180 MeV). For each closed orbit, coordinates are stored in orbits.fai file (at MARKER with LABEL1=afterFIT right after the FIT, prior to REBELOTE repeat).

The input data file ends with a SYSTEM command which, once zgoubi is done with finding/storing the periodic orbits, launches a subsequent computation ("cd tempo; ./zgoubi -in plotOrbits.dat" command) which performs the following:

- first, the periodic orbit coordinates are read from orbits.fai,

- they are then pushed through the magnet, and the trajectories are logged in zgoubi.plt (the effect of IL=2 under FFAG) for further post-tratment or plotting.

A plot is launched by the next two gnuplot commands under SYSTEM, outcomes are displayed in Fig. 20.95.

A plot of orbits around the ring can be obtained from the previous raytracing, for instance using a loop in gnuplot to increment the polar angle by steps of 36 deg, reading particle data across the cell from zgoubi.plt; it is displayed in Fig. 20.96.

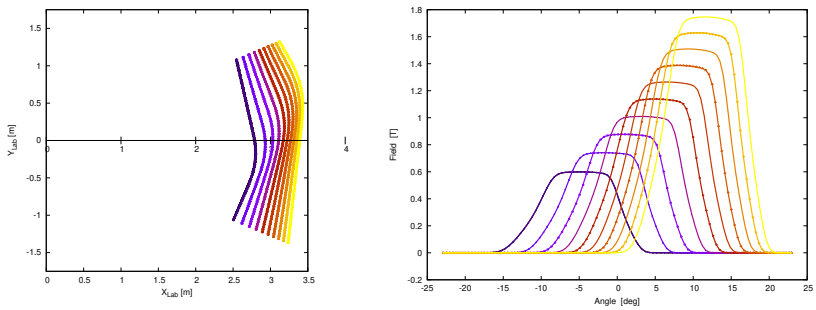

Fig. 20.95 Periodic orbits and field across RACCAM FFAG spiral sector dipole. Left: orbit scalloping across AT=45.83° arc extent in FFAG-SPI simulation (a cell is 36°), for different proton energies ranging in 15-180 MeV. Right: field experienced along these orbits, increasing with energy

(b) Homothety-rotation of the orbits.

The orbit scalloping is apparent in Fig. 20.95 and Fig. 20.96. Step By Step values can be drawn from zgoubi.plt and show that the scalloping $\delta R/R$ is in the % range. Rotation of the closed orbit pattern in also apparent in Figs. 20.95, 20.96; the radius dependence of the rotation angle satisfies Eq. 11.13. The expected value from the latter can be checked against closed orbit data logged in zgoubi.plt.

(c) Figure 20.97 compares the numerical and theoretical (Eq. 11.8) values of the average orbit radius $R = C/2\pi$, both in good accord.

Table 20.80 Simulation input data file: find the closed orbit for a set of different momenta. The INCLUDE is the FFAG-SPI spiral dipole segment from Tab. 20.79, within LABEL1s #*S_RACCAMCell* and #*E_RACCAMCell*

```
Orbit scan.
'MARKER'  RACCAMProbOrbits_S                                              ! Just for edition purposes.
'OBJET'
2029.47926                                                          !  Reference rigidity (180MeV proton).
2
1  1
2.848940E+02  3.005184E+02  0.0E+00  0. 0.  0.276852600 'i'                            ! 15 MeV proton.
1
'PARTICUL'
PROTON
'FAISTORE'
orbits.fai afterFIT  ! Coordinates are saved in orbits.fai. This is effective at 'afterFIT' label, below.
1

'INCLUDE'                                                    ! Include the 36 degree spiral sector dipole,
1                                                                          ! within dedicated  LABEL1s.
./RACCAMCell.inc[#S_RACCAMCell:#E_RACCAMCell]

 'FIT2'
2  nofinal
2 30 0  2.
2 31 0  2.
2  1e-9 99                                                        ! A penalty value controls the accuracy
3.1 1 2 #End 0. 1. 0                                          ! of the convergence to periodic coordinates.
3.1 1 3 #End 0. 1. 0                                               ! 3.1 is the constraint for periodicity.
'MARKER' afterFIT                                                          ! FAISTORE above applies here.

'REBELOTE'                                                                ! Repeat the previous sequence,
10 0 0  1                                                                  ! 10 times; prior to repeating, change
1                                                             ! 1 parameter: parameter 35 under OBJET, namely,
OBJET 35 0.276852600:1.                ! the relative momentum, D=p/p_ref, in the range  0.276852600:1.

'SYSTEM'
6
(mkdir -p tempo;  cp zgoubi.res tempo/temp.res; cp orbits.fai tempo)             ! In a separate folder,
ln -s /home/meot/zgoubi/current/zgoubi/zgoubi                          ! establish a link to zgoubi executable,
(cp  plotOrbits.dat tempo ; cd tempo; ./zgoubi -in plotOrbits.dat)           ! track orbits using initial
mv tempo/zgoubi.plt .                                                      ! coordinates as read from orbits.fai.
gnuplot <./gnuplot_Zplt_XY.gnu                    ! Call gnuplot scripts once that tracking is completed.
gnuplot <./gnuplot_Zplt_XB.gnu

'MARKER'  RACCAMProbOrbits_E                                              ! Just for edition purposes.
'END'
```

plotOrbits.dat file, to track orbits using initial coordinates as read from orbits.fai (note: in the sub-folder 'tempo', a link to zgoubi executable is required to run this file):

```
plotOrbits.dat
 'OBJET'
2029.47926                                                          !  Reference rigidity (180MeV proton).
3
1 999 1
1 999 1
1. 1. 1. 1. 1. 1. 1. '*'
0. 0. 0. 0. 0. 0. 0.
0
orbits.fai

'INCLUDE'
1
./temp.res[#S_RACCAMCell:#E_RACCAMCell]

'FAISCEAU'
'END'
```

---

gnuplot scripts gnuplot_Zplt_XY.gnu and gnuplot_Zplt_XB.gnu, for Fig. 20.95:

```
#gnuplot_Zplt_XY.gnu
set xtics mirror ; set ytics mirror ; set xlabel "X_{Lab} [m]" ;set ylabel "Y_{Lab} [m]"
set polar; unset colorbox; cm2m = 0.01; set xrange [0:3.5]; set yrange [-1.75:1.75]; set size square
plot for [i=2:11]  "zgoubi.plt" u ($22):(cm2m* $10):($19) w p ps .4  lc palette notit; pause 1

#gnuplot_Zplt_XB.gnu
set xtics mirror ; set ytics mirror
set xlabel "Angle  [deg]"  ; set ylabel "Field  [T]"
r2d = 180./ (4.*atan(1.)) ; kG2T=0.1
plot for [i=1:11] "zgoubi.plt" u ($19== i ? $22 *r2d : 1/0):($25 *kG2T) w lp lw 2 ps .2 notit; pause 1
```

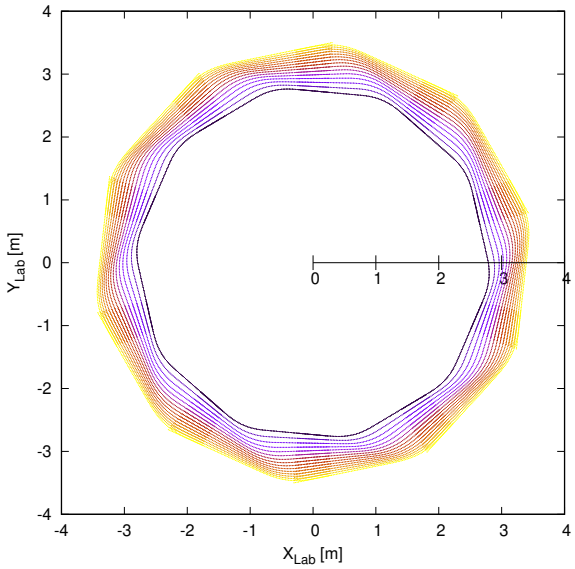

Fig. 20.96 Fifteen closed orbits around the 10-cell spiral sector RACCAM ring, in the range 15 to 180 MeV

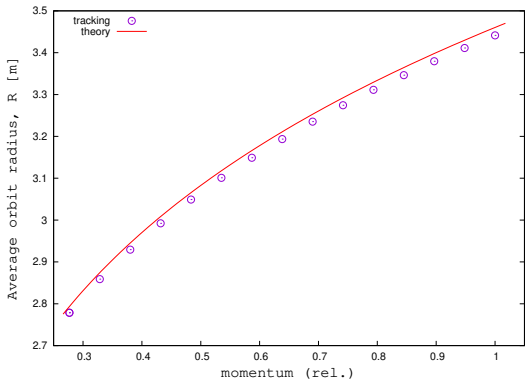

Fig. 20.97 Dependence of the average closed orbit radius $R = C/2\pi$ on the relative momentum. Markers are from one-turn raytracing. The solid line is from theory, for comparison, after Eq. 11.8 taken for $k = 5$ (Tab. 11.2) and reference momentum $p_{\mathrm{ref}} = 608.422$ MeV/c (180 MeV, radius $R_0 = 3.46031$ m). They only differ by $\approx 1\%$

11.8

Zero-Chromaticity

(a) Momentum dependence of tunes.

The input data file in Tab. 20.81 computes momentum-dependent transport matrices of the cell, $[T_{ij}](p)$, for a series of different momenta.

Table 20.81 Simulation input data file: compute the first order transport matrix of the cell for a series of momenta. Prior to matrix computation, the closed orbit is found by FIT, or FIT2. The INCLUDE is the FFAG-SPI spiral dipole segment from Tab. 20.79, within LABEL1s $\#S\_SFFAG150Cell$ and $\#E\_SFFAG150Cell$

```
Scan transport matrix of 180 MeV RACCAM cell
 'OBJET'
2029.47926                                                    ! Reference rigidity, 180 MeV proton.
5                                                                 ! Option for MATRIX computation.
.01 .001 .01 .001 0. 0.0001                                ! 13-trajectory sampling for MATRIX computation.
284.894   300.516 0. 0. 0. 0.276852600  'o'               ! Reference trajectory (number 1 in the 11-set).
1

'INCLUDE'                                                    ! Include the 30 degree sector dipole triplet,
1                                                                          ! within dedicated  LABEL1s.
./RACCAMCell.inc[#S_RACCAMCell:#E_RACCAMCell]

 'FIT2'
2  noFinal
1 30 0  2.
1 31 0  2.
2  1e-6 79                                          ! A penalty value, 1e-9 here, controls the accuracy
3.1 1 2 #End 0. 1. 0                          ! of the convergence of the constraints to the target values.
3.1 1 3 #End 0. 1. 0                                        ! 3.1 is the constraint for periodicity.

'MATRIX'
1 11  PRINT                              ! PRINT causes log of transport coefficients to zgoubi.MATRIX.out.

'REBELOTE'                                                                ! Repeat the previous sequence,
20 0 0  1                                                          ! 20 times; prior to repeating, change
1                                                          ! 1 parameter: parameter 35 under OBJET, namely,
OBJET 35 0.276852600:1.                 ! the relative momentum, D=p/p_ref, in the range  0.276852600:1.

'SYSTEM'
1
gnuplot <./gnuplot_tunes.gnu                       ! Gall gnuplot script once that tracking is completed.
 'END'
```

gnuplot script for Fig. 20.98:

```
# gnuplot_tunes.gnu
system "grep 'Fit reached penalty value ' zgoubi.res | cat > grep.out"  # extract penalty values from zgoubi.res
plot "zgoubi.MATRIX.out" u (0+$47):(Ncell* $56) w  p  pt 6 ps .9 tit "{/Symbol}_R", \
"zgoubi.MATRIX.out" u (0+$47):(Ncell* $57) w  p  pt 7 ps .9 tit "{/Symbol}_Z",  \
(x<1.03 ? sqrt(1+k) :1/0) w l lw 2 tit "\sqrt{(1+k)}" ,  "grep.out" u :5 axes x2y2  ; pause 1
```

OBJET with option KOBJ=5 defines a set of 13 particles with proper initial coordinates for matrix computation, by MATRIX. Prior to matrix computation, the momentum-dependent closed orbit is found by FIT. REBELOTE changes the relative momentum D in OBJET, and repeats the procedure. The PRINT command under MATRIX logs the transport coefficients to zgoubi.MATRIX.out, together with the beam matrix and tunes which are obtained from the hypothesis of periodicity (the argument '11' under MATRIX), namely from the identification [1, Sect. 6.5.6]

$$[T_{ij}] = I \cos\mu + J \sin\mu$$

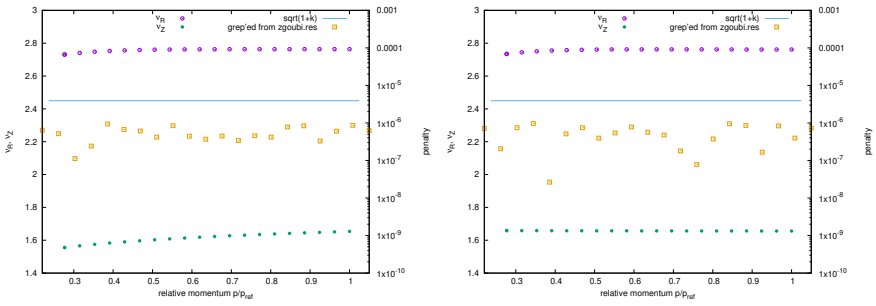

Fig. 20.98 Radial (ν_R) and axial (ν_Z) tunes of the 10-cell ring (left vertical scale), as a function of relative momentum ($p/p_{\rm ref} = 1$ for 180 MeV). The penalty values (scattered squares, right vertical scale) monitor the FIT runs, they have to be small to confirm the convergence of FIT. Left: case of slowly increasing gap height (thus increasing fringe extent) with radius: $g(R) = g_0 \left(\frac{R_0}{R}\right)^{-0.52}$. Right: case of linear increase of gap height (thus linear increasing of fringe extent) with radius: $g(R) = g_0 \left(\frac{R}{R_0}\right)$

These data are then read and plotted (Fig. 20.98). The radial tune ν_R is constant (apart from a slight depression towards lower momenta where the dipole width reduces due to the spiral shape) as expected from the zero-chromaticity resulting from the scaling law (momentum-independent index, Eq. 11.3). Such is not the case for the axial tune, ν_Z, due to the first order effect of fringe field extent on the axial focusing (see Sect. 18.3.1): fringe extent varies with orbit radius in correlation with a simulated gap height $g(R) \propto 1/R^\kappa$ ($\kappa = -0.52$), too slow an increase of g with radius for proper chromaticity compensation.

(b) R-dependence of axial tune.

The variation of the axial tune with momentum, as observed in (a), is due to the fact that the fringe field extent does not increase fast enough with radius. Indeed the gap shape index in the present spiral sector model is $\kappa = -0.52$ (Tab. 20.79), resulting, in the FFAG-SPI modeling, in a gap height

$$g(R) = g_0 \left(\frac{R}{R_0}\right)^{0.52}$$

whereas constant wedge angle focusing requires $\kappa = -1$, namely [2, 3]

$$g(R) = g_0 \left(\frac{R}{R_0}\right)$$

(c) Constant axial tune.

The axial tune is made constant using a gap law (Eq. 11.6) with $\kappa = -1$, namely, gap height proportional to R [2, 3]. The simulation is obtained by changing the lines concerned in FFAG-SPI keyword input data list (Tab. 20.79), namely

change “8.95 – 0.52 ! EFB [etc.]” to “8.95 – 1. ! EFB [etc.]”

at the 2 EFBs. The resulting tunes, for this $g(R) \propto R$ gap shape, are displayed in Fig. 20.88.

(d) Momentum compaction and transition γ_{tr}

TWISS keyword is used to compute various first and second order optical parameters - it does a little more than MATRIX, and similarly uses the 13-particle OBJET[KOBJ=5]. A typical input file including TWISS is given in Tab. 20.82. Results are given in Tab. 20.83.

The momentum compaction is expected to satisfy $\alpha = \frac{\Delta C}{C} / \frac{\Delta p}{p} = 1/(1+k)$. In the present design $k = 5$, yielding $\alpha = 0.1666$. This approximation is acceptable at high energy where computed $\alpha = 0.1666$ (Tab. 20.83), very close to $1/(1+k)$, however it is not at low energy where the numerical integration yields $\alpha = 0.60173$.

Table 20.82 Simulation input data file: TWISS command, to obtain the periodic beam matrix, momentum compaction, chromaticities, etc. The initial reference coordinates, under OBJET, are for 15 MeV. TWISS proceeds in 3 stages: it first computes tunes of an on-momentum particle, then for $\pm\delta p/p$ off-momentum particles; at each stage, FIT ensures that the reference particle (1st particle of the 11-set) is on the closed orbit. The INCLUDE uses the segment #S_RACCAMCell to #E_RACCAMCell defined in Tab. 20.79

```
RACCAM cell, TWISS computation
'MARKER' RACCAM_TWISS_S
 'OBJET'
2029.47926                                                    ! Reference rigidity, 180 MeV proton.
5                                                                 ! Option for MATRIX computation.
.01 .001 .01 .001 0. 0.0001                              ! 13-trajectory sampling for  TWISS computation.
284.894   300.516 0. 0. 0. 0.276852600  'o'             ! Reference trajectory (number 1 in the 11-set).
1

'INCLUDE'                                                   ! Include the 30 degree sector dipole triplet,
1                                                                          ! within dedicated  LABEL1s.
./RACCAMCell.inc[#S_RACCAMCell:#E_RACCAMCell]

 'FIT2'                                                        ! Find closed orbits, on- and off-momentum.
2  noFinal
1 30 0  2.
1 31 0  2.
2  1e-6 79                                          ! A penalty value, 1e-9 here, controls the accuracy
3.1 1 2 #End 0. 1. 0                        ! of the convergence of the constraints to the target values.
3.1 1 3 #End 0. 1. 0                                    ! 3.1 is the constraint for periodicity.

'TWISS'
2 1. 1.
'MARKER' RACCAM_TWISS_E
'END'
```

Table 20.83 Outcomes of TWISS computation out of zgoubi.res listing, including beam matrix, tunes, momentum compaction factor, and near-zero chromaticities

Case of 15 *MeV optics*:

```
Reference, before change of frame (particle #  1  - D-1,Y,T,Z,s,time)  :
-7.23147400E-01   2.84894063E+02   3.00515234E+02   0.00000000E+00   0.00000000E+00   1.74585982E+02   3.29572993E-02

Reference, after change of frame (particle #  1  - D-1,Y,T,Z,s,time)  :
-7.23147400E-01   0.00000000E+00   0.00000000E+00   0.00000000E+00   0.00000000E+00   1.74585982E+02   3.29572993E-02

               TRANSFER  MATRIX  ORDRE  1  (MKSA units)
      -0.881744        0.852462         0.00000         0.00000         0.00000         0.685431
       -1.75188        0.559596         0.00000         0.00000         0.00000         0.358061
        0.00000         0.00000        -1.16322         3.85003         0.00000         0.00000
        0.00000         0.00000       -0.950162         2.28518         0.00000         0.00000
       0.575188       -7.833153E-02     0.00000         0.00000         1.00000         4.164093E-02
        0.00000         0.00000         0.00000         0.00000         0.00000         1.00000

     DetY-1 =      -0.0000068160,    DetZ-1 =      -0.0000160216

    Beam  matrix  (beta/-alpha/-alpha/gamma) and  periodic  dispersion  (MKSA units)
        0.863743     0.730208     0.000000     0.000000     0.000000     0.261440
        0.730208     1.775068     0.000000     0.000000     0.000000    -0.226953
        0.000000     0.000000     4.650813     2.082825     0.000000    -0.000000
        0.000000     0.000000     2.082825     1.147791     0.000000     0.000000

                        Betatron  tunes  (Q1 Q2 modes)
                NU_Y =  0.27574797         NU_Z =  0.15521091

                        Momentum compaction :
                dL/L / dp/p =  0.59900604

                        Chromaticities :
              dNu_y / dp/p = -1.70372346E-03              dNu_z / dp/p =  7.26717831E-03
```

Case of 180 *MeV optics*:

```
Reference, before change of frame (particle #  1  - D-1,Y,T,Z,s,time)  :
 0.00000000E+00   3.36987609E+02   9.05358647E+00   0.00000000E+00   0.00000000E+00   2.16232505E+02   1.32569144E-02

Reference, after change of frame (particle #  1  - D-1,Y,T,Z,s,time)  :
 0.00000000E+00   0.00000000E+00   0.00000000E+00   0.00000000E+00   0.00000000E+00   2.16232505E+02   1.32569144E-02

               TRANSFER  MATRIX  ORDRE  1  (MKSA units)
       0.551741         1.04666         0.00000         0.00000         0.00000        0.485854
       -1.42011       -0.881528         0.00000         0.00000         0.00000        0.359691
        0.00000         0.00000       -0.446750         2.01463         0.00000         0.00000
        0.00000         0.00000       -0.820807         1.46308         0.00000         0.00000
       0.879375        0.804775         0.00000         0.00000         1.00000        5.070098E-02
        0.00000         0.00000         0.00000         0.00000         0.00000         1.00000

     DetY-1 =      -0.0000041477,    DetZ-1 =      -0.0000094508

    Beam  matrix  (beta/-alpha/-alpha/gamma) and  periodic  dispersion  (MKSA units)
        1.061187    -0.726582     0.000000     0.000000     0.000000     0.553967
       -0.726582     1.439822     0.000000     0.000000     0.000000    -0.226945
        0.000000     0.000000     2.339177     1.108747     0.000000    -0.000000
        0.000000     0.000000     1.108747     0.953036     0.000000     0.000000

                        Betatron  tunes  (Q1 Q2 modes)
                NU_Y =  0.27636408         NU_Z =  0.16516182

                        Momentum compaction :
                dL/L / dp/p =  0.16657894

                        Chromaticities :
              dNu_y / dp/p =  4.34427556E-04              dNu_z / dp/p =  7.34661292E-03
```

11.9

Beam Envelopes, Optical Functions

Beam envelopes can be obtained by single particle raytracing over a few tens of passes through a cell. A proper data file for that is given in Tab. 20.84, it uses OBJET[KOBJ=2] to define the particle.

Multiturn raytracing results are given in Fig. 20.99, which also displays the square of the transverse particle excursion, normalized to the motion invariant, to yield betatron function amplitudes, namely, $\beta_Y = Y^2/\varepsilon_Y/\pi$ and $\beta_Z = Z^2/\varepsilon_Z/\pi$.

An alternate technique to get the optical functions at all s across the cell is by transporting the beam matrix from the origin (s_0)

$$\sigma(s) = T(s \leftarrow s_0)\,\sigma(s_0)\,\tilde{T}(s \leftarrow s_0)$$

The transport matrix $T(s \leftarrow s_0)$ can be computed step by step from the particle coordinates stored in zgoubi.plt during the raytracing. A tool in zgoubi toolbox does that, betaFromPlt [7], it requires using the 13-particle OBJET[KOBJ=5], and logging stepwise particle data in zgoubi.plt. This method is used in solving exercise **??** (Fig. **??**).

Table 20.84 Simulation input data file: raytrace two particles with different momenta through a cell, over 110 passes. Initial radial and axial coordinates are taken on $\varepsilon_{Y,Z}/\pi = 10^{-8}$ m invariants. The INCLUDE uses the segment [#S_RACCAMCell:#E_RACCAMCell] defined in Tab. 20.79

```
Track beam envelops
'OBJET'
2029.47926                                                              ! Rigidity of 180 MeV proton.
2
2 1
2.84903389E+02 300.593197 2.1566E-02 9.658E-02 0. 0.2768526 'o'    !  15 MeV, on 1e-8m Y nd Z invariants.
3.37019202E+02 8.84910511 1.5294E-02 7.249E-02 0.  1.       'i'    ! 180 mEv, on 1e-8m Y nd Z invariants.
1 1

'INCLUDE'                                                 ! Include the 30 degree sector dipole triplet,
1                                                                  ! within dedicated  LABEL1s.
./RACCAMCell.inc[#S_RACCAMCell:#E_RACCAMCell]

'REBELOTE'                        ! Repeat sequence 109 times; '0.1': log pass-by-passes count to video;
109 0.1 99                                                 ! '99': ignore OBJET at subsequent passes.
'END'
```

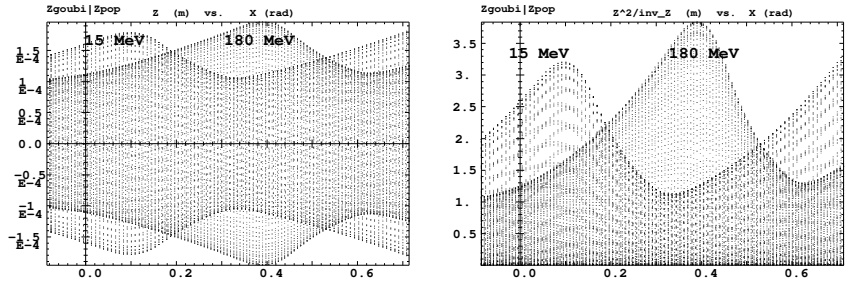

Fig. 20.99 Left: axial excursion of two particles, one 15 MeV and the other 180 MeV, over 110 passes across a 45.83° arc (the extent of the field region, AT, in FFAG-SPI, whereas a period is 36°). Both particles are taken on a axial invariant $\varepsilon_Z/\pi = 10^{-8}$ m. This multiple pass plot generates the beam envelopes, namely, the loci of the extrema of particle excursion. Right: the graph shows $Z(s)^2/\varepsilon_Z$, with Z(s) particle motion from the left and $\varepsilon_Z/\pi = 10^{-8}$ m the motion invariant. The loci of the extrema are the betatron function amplitudes. These graphs are obtained using the interface program zpop, to plot from zgoubi.plt storage file (left plot: menu 7; 1/1 to open zgoubi.plt; 2/[8,4] to select Z versus X (azimuthal angle); 7 to plot; right plot: chose menu 7: 3/14 to change the axial coordinate to Z^2/constant)

11.10

Periodic Stability Domain The stability domain in the tune diagram, and the corresponding (k, ζ) domain, are obtained by a (k, ζ) scan, performed for some arbitrary momentum, for instance half-way between injection and top energy. A similar simulation input data file to that in Tab. 20.81 is used. The process is the following:

(1) a FIT and MATRIX sequence finds closed orbit and related tunes, for a given (k, ζ) value,

(2) REBELOTE then varies k and repeats the FIT & MATRIX sequence (1),

(3) from that scan results a series of (ν_R, ν_Z) couples, corresponding to a series of (k, ζ) couples at fixed spiral angle ζ,

This (1)-(3) sequence is repeated for a series of ζ values - an external program can be used to perform that iteration on ζ.

This results in (k, ζ) and (ν_R, ν_Z) stability diagrams displayed in Fig. 20.100. The correlation comes out to be, mostly, an increase of ν_R with k and increase of ν_Z with ζ, however the two quantities are not fully decoupled, increasing k (respectively, ζ) has a slight effect on ν_Z (resp. ν_R). A comparison with matrix product techniques (using a matrix code) shows the interest of stepwise raytracing in realistic field models, for accuracy.

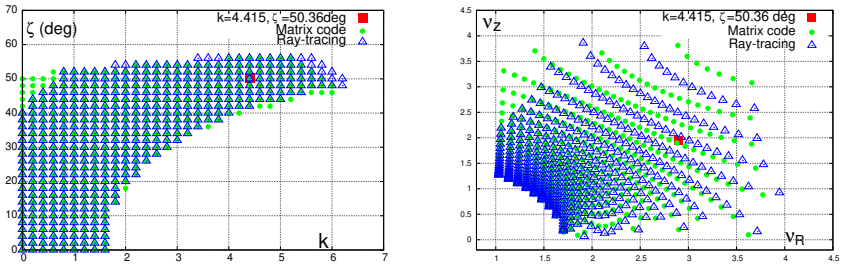

Fig. 20.100 A scan of k and ζ. Left: (k, ζ) stability domain, right: corresponding (ν_R, ν_Z) stability domain. In both diagrams a particular working point, $(k, \zeta) = (4.415, 50.36)$, is shown for illustration (different from the working point in these exercises, which is $(k, \zeta) = (5, 53.7)$)

11.11

Motion Stability Limit

The input data file in Tab. 20.85 can be used:

- raytracing is performed for one particle at a time (namely, for a particular energy taken in [15 MeV,180 MeV])

- REBELOTE performs a multiturn raytracing

Then push the initial coordinate (Y_0 for radial stability limit, Z_0 for axial), up to stability limit. An external program available in zgoubi toolbox, searchStabLim, does that and can be used instead [8].

This will result in phase space portraits similar to Fig. 11.15 as to the radial stability limits, and Fig. 20.101 as to the axial stability limits.

Table 20.85 Simulation input data file: track one particle, for 1000 turns. Push Y_0 up to find the stability limit. Using the complete ring (10 cells) allows introducing non-systematic errors if desired (random field or positioning errors for instance, using ERRORS keyword). If only systematic errors or non-linearities are of interest, then a single cell is enough, and the 1000-turn tracking is set 10,000 passes instead

```
Track one particle
'OBJET'
2029.47926                                                    ! Rigidity of 180 MeV proton.
2
2 1
284.894   300.516 0. 0. 0. 0.276852600  'o'             ! Reference trajectory (number 1 in the 11-set).
1 1
'INCLUDE'                                                   ! Include the 30 degree sector dipole triplet,
1                                                                ! within dedicated  LABEL1s.
10* ./RACCAMCell.inc[#S_RACCAMCell:#E_RACCAMCell]                ! 10 cells, a complete ring.
'REBELOTE'                  ! Repeat sequence 999 times; '0.3': log count every other 100 pass to video;
999 0.3 99                                                  ! '99': ignore OBJET at subsequent passes.
'END'
```

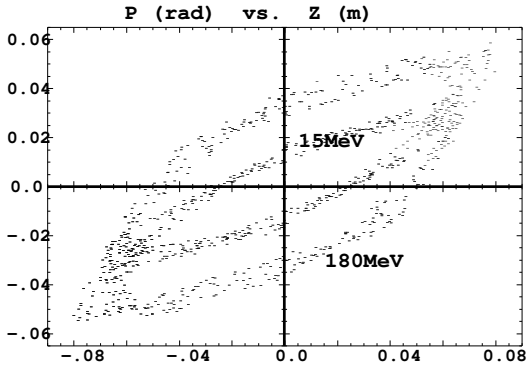

Fig. 20.101 Stability limit in the axial phase space, at 15 MeV (smaller ellipse) and 180 MeV (quadrilateral shaped portrait). The distortion of these large invariants is due to field non-linearities, their spreading is due to non-linear coupling

11.12

Dynamic Aperture Scan

A DA scan is obtained by repeating the previous (exercise 11.11) stability limit search:

- first, look for the maximal radial extent $[x_{\min}, x_{\max}]$ of stable horizontal motion, at quasi-zero axial invariant,

- second, look for the maximum stable axial amplitude, at various values $x \in [x_{\min}, x_{\max}]$.

An external program available in zgoubi toolbox does that, searchDA [9]. The exercise results in the DA graph of Fig. 20.102.

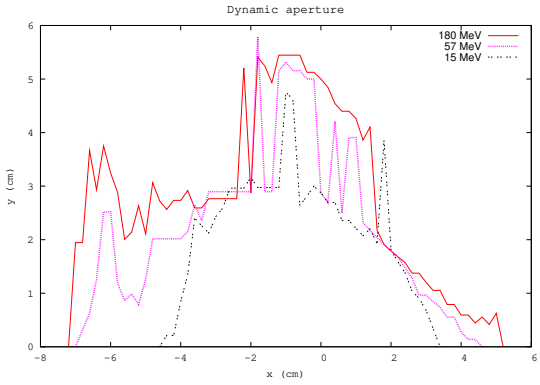

Fig. 20.102 Dynamic aperture in the (Y,Z) space. Stable horizontal motion (at quasi-zero axial motion) depends on momentum of concern; the origin here, x=0, is on the closed orbit at that energy

11.14

Acceleration, Adiabatic Damping

Setting up the acceleration requires the following:

- CAVITE boosts the particle(s) at each pass,

- PARTICUL/PROTON is necessary as CAVITE is used: it allows converting energy change in rigidity change (zgoubi pushes particles using rigidity),

- SCALING, akin to a "power supply rack", provides the RF program to CAVITE (by reading it from an external file, zgoubi.freqLaw.In),

- REBELOTE sends the execution pointer back to the top of the input data file, for multiturn tracking. A 10 kV acceleration rate per turn may be obtained from constant peak voltage $\hat{V} = 20\,\mathrm{kV}$ and synchronous phase $\phi_s = 30°$, this determines the number of passes for a 15→180 MeV cycle, namely, $(180 - 15)/0.01 = 16500$ (hence a number of repeat of 16499 under REBELOTE),

- FAISTORE stores turn-by-turn particle data (to some user defined file, *e.g.* zgoubi.fai).

For simplicity the RF program may be limited to the turn dependence of RF frequency (peak voltage and synchronous phase maintained constant). Elaborating zgoubi.freqLaw.In (essentially two columns: RF frequency versus turn number) requires the following steps (exercise 11.5 may also be referred to, see zgoubi.freqLaw.In file formatting and sample content in Tab. 20.78):

(i) run a search for closed orbits for a few tens of energies in the range 15 to 180 MeV. Time of flight, derived from path length and particle velocity, is part of the outcome of orbit computation as PARTICUL provides necessary particle data in that aim. That yields the turn dependence of RF frequency, namely, $f_{\mathrm{RF}} = h \times f_{\mathrm{rev}} = v/C$ (assuming RF harmonic h=1). Note that in the absence of orbit defects or other tailored bumps, the frequency law may be obtained instead from the theoretical orbit length $C(p) = C_0(p/p_0)^{\frac{1}{k+1}}$ (Eq. **??**), as it is expected to yield similar values to the aforementioned closed orbit raytracing outcomes;

(ii) store these turn-frequency data, properly formatted, in zgoubi.freqLaw.In. Note that zgoubi.freqLaw.In does not need to contain all turns, zgoubi will interpolate from what is found therein.

The resulting radial and axial phase spaces are displayed in Fig. 20.103. The betatron damping satisfies Eqs. 11.21, 11.22. The homothety-rotation of the geometrical scaling is apparent in the axial phase space portrait.

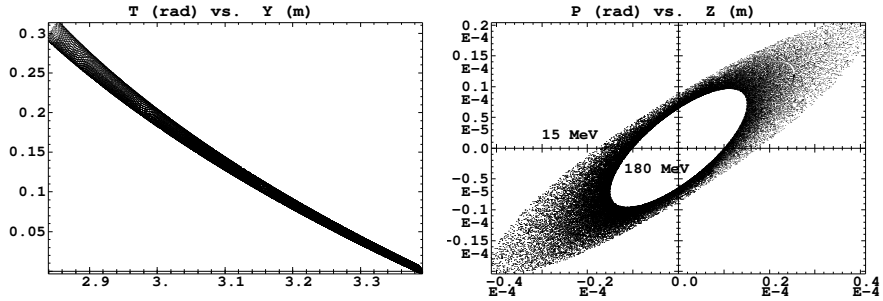

Fig. 20.103 Acceleration from 15 to 180 MeV. Radial and axial phase spaces. These graphs are obtained using the interface program zpop, which reads turn-by-turn particle coordinates from zgoubi.fai (menu 7; 1/5 to open zgoubi.fai; 2/[2,3] to select T (angle) versus Y (radius) [or 2/[4,5], for P versus Z]; 7 to plot)

20.6.3 FFAG Acceleration Methods

Regarding the lattice, the following three execises are based on a very similar radial sector triplet FFAG to that studied in detail in the Sect. 11.3.1 exercise series. Thus earlier simulation input data files can be used here, and will only require minor adaptations.

Regarding beam acceleration, the input data files and methods developed in the previous exercises (exercises 11.5, 11.13, 11.14) can be used to set up the present acceleration simulation input data.

11.15

Hybrid Acceleration

Refer to [11, 12] where all necessary details regarding working hypotheses, and partial results, including numerical simulations, can be found.

11.16

Bucket Acceleration

Refer to [13] where all necessary details regarding working hypotheses, and partial results, including numerical simulations, can be found.

Regarding in-flight decay method and outcomes, refer to the exercises in Sects. 15.3.3, 15.3.4.

11.17

Serpentine Acceleration

Refer to [14, 15] where all necessary details regarding working hypotheses, and partial results, including numerical simulations, can be found.

References

1. Méot, F.: Zgoubi Users' Guide. https://www.osti.gov/biblio/1062013-zgoubi-users-guide An up-to-date version of the guide: https://sourceforge.net/p/zgoubi/code/HEAD/tree/trunk/guide/Zgoubi.pdf
2. Antoine, S. et al.: Principle design of a proton therapy, rapid-cycling, variable energy spiral FFAG, NIM A 602 (2009) 293-305.
3. Planche, T., et al.: Design of a prototype gap shaping spiral dipole for a variable energy proton therapy FFAG. NIMA 604 (2009) 435-442.
4. Méot, F., Lemuet, F.: Developments in the ray-tracing code Zgoubi for 6-D multiturn tracking in FFAG rings. NIM A 547 (2005) 638-651.
5. Fourrier, J., Martinache, F., Méot, F., Pasternak, J.: Spiral FFAG lattice design tools,application to 6-D tracking in a proton-therapy class lattice. NIM A 589 (2008) 133-142.
6. Méot, F.: RACCAM: a status including magnet prototyping and magnetic measurements. International conference on FFAGs, Fermilab, 21-25 September 2009. https://indico.fnal.gov/event/2672/session/2/contribution/8/material/slides/
7. From zgoubi toolbox, part of the sourceforge package: a Fortran tool to compute optical functions from a zgoubi.plt output file, and some related gnuplot scripts: https://sourceforge.net/p/zgoubi/code/HEAD/tree/trunk/toolbox/betaFromPlt/
8. From zgoubi toolbox, part of the sourceforge package: a Fortran tool to perform a dynamic aperture scan, and some related gnuplot scripts: https://sourceforge.net/p/zgoubi/code/HEAD/tree/trunk/toolbox/searchStabLim/
9. From zgoubi toolbox, part of the sourceforge package: a Fortran tool to perform a dynamic aperture scan, and some related gnuplot scripts: https://sourceforge.net/p/zgoubi/code/HEAD/tree/trunk/toolbox/searchDA/
10. Prior, C.: High Intensity Proton Studies at RAL. Oral presentation, TUP1WA01, HB2018 Workshop, Daejeon, Korea (June 18-22, 2018). http://accelconf.web.cern.ch/AccelConf/hb2018/ // Lagrange, J. B., et al.: Progress on Design Studies for the ISIS II Upgrade. TUPTS068, IPAC2019, Melbourne, Australia (19 âĂŞ 24 MAY 2019). http://accelconf.web.cern.ch/AccelConf/ipac2019/papers/tupts068.pdf
11. Tanaka, H.: Feasibility Study of Hybrid Accelerator and Superconducting FFAG. FFAG04 Accelerator Workshop, KEK, Tsukuba (October 13-16, 2004). http://130.246.92.181/FFAG/FFAG04_HP/index.html
12. Tanaka, H., et al.: Hybrid Accelerator Using an FFAG Injection Scheme. Cyclotrons 2004 Conf., Tokyo, Japan (18-22 Oct 2004). http://accelconf.web.cern.ch/AccelConf/c04/data/CYC2004_papers/19C6.pdf
13. Planche, T., et al.: New Approaches to Muon Acceleration With Zero-Chromatic FFAGs. THPD093, Proceedings of IPACâĂŹ10, Kyoto, Japan (2010). http://accelconf.web.cern.ch/AccelConf/IPAC10/papers/thpd093.pdf
14. Yamakawa, E.: Serpentine Acceleration in Zero-chromatic FFAG with Long Straight Section. International Workshop on FFAG Accelerator (FFAG'10) Kyoto University Research Reactor Institute, Osaka, Japan (28-31 October 2010). http://130.246.92.181/FFAG/FFAG10_HP/slides/Sat/Sat14Yamakawa.pdf
15. Yamakawa, E., et al.: Serpentine acceleration in zero-chromatic FFAG accelerators. Nuclear Instruments and Methods in Physics Research Section A: Accelerators, Spectrometers, Detectors and Associated Equipment, Volume 716, 11 July 2013, Pages 46-53